RISK BASED APPROACH TO PREDICT CASING LEAKS USING ELECTROMAGNETIC CORROSION LOGS

BY

Mohammed Dhafer Mohammed Al-Ajmi

A Thesis Presented to the
DEANSHIP OF GRADUATE STUDIES

KING FAHD UNIVERSITY OF PETROLEUM & MINERALS

DHAHRAN, SAUDI ARABIA

In Partial Fulfillment of the
Requirements for the Degree of

MASTER OF SCIENCE

In

PETROLEUM ENGINEERING

January 2017

KING FAHD UNIVERSITY OF PETROLEUM & MINERALS

DHAHRAN- 31261, SAUDI ARABIA

DEANSHIP OF GRADUATE STUDIES

This thesis, written by **Mohammed Dhafer Mohammed Al-Ajmi** under the direction his thesis advisor and approved by his thesis committee, has been presented and accepted by the Dean of Graduate Studies, in partial fulfillment of the requirements for the degree of **MASTER OF SCIENCE IN PETROLEUM ENGINEERING**

Dhafer A. Al-Shehri

Dr. Dhafer A. Al-Shehri
(Advisor)

Dr. Abdullah S. Sultan
Department Chairman

Mohamed Mahmoud

Dr. Mohamed A. Mahmoud
(Member)

Dr. Salam A. Zummo
Dean of Graduate Studies

DEANSHIP OF GRADUATE STUDIES

Dr. Abdulaziz Abdulraheem
(Member)

22/2/17

Date

This work is dedicated to my dear wife Loubna

ACKNOWLEDGMENTS

I would like to thank King Fahd University of Petroleum & Minerals and all its staff for their continued support to complete my master degree. Special thanks go to my dear professor and thesis advisor Dr. Dhafer Al-Shehri for his guidance throughout this research period. Thesis committee Dr. Mohammed Mahmoud and Dr. Abdulaziz Abdulraheem are deeply appreciated for their helpful contribution to complete my thesis work.

I would like to my family. My parents, spouse, brothers and sisters for their kind love and words of encouragement.

To my father, you have always been and will always be my source of inspiration. I thank you heartedly for that.

TABLE OF CONTENTS

LIST OF TABLES

ABSTRACT

Full Name : Mohammed Dhafer Mohammed Al-Ajmi

Thesis Title : Risk-Based Approach to Predict Casing Leaks Using Electromagnetic Corrosion Logs

Major Field : Petroleum Engineering

Date of Degree : January 2017

This research has entertained and scrutinized several challenges faced by the petroleum industry in the field of wellbore integrity, downhole corrosion growth and multiple casings' metal loss assessment with more focus on cutting-edge electromagnetic corrosion logging technology. Engineering solutions, innovative approaches and risk-based casing failures prediction models were formulated to address these challenges. These solutions will have significant impact on improving field safety (assets and personnel), mitigating wellbore risks and optimizing operational economics through data-driven well integrity surveillance. The research outcomes, data analysis, and prediction models are based on an extensive review of more than five hundred case studies from multiple Saudi Arabian fields.

In addition, the research included a comprehensive review of well integrity surveillance technology evolution and impact on well integrity management strategy in mature oil and gas fields.

The general objectives of this research work are outlined as follows:

- Formulating a probabilistic model to predict downhole casing leaks based on electromagnetic corrosion logging data.

- Establishing guidelines to design a cost-effective casing integrity surveillance program based on electromagnetic corrosion logging analysis outcomes.

ملخص الرسالة

الاسم الكامل: محمد ظافر محمد العجمي

عنوان الرسالة: مقاربة مبنية على تقدير المخاطر للتنبؤ بتسريبات الهيكل الداخلي للآبار النفطية باستخدام سجلات التآكل الكهرومغناطيسية

التخصص: هندسة البترول

تاريخ الدرجة العلمية: يناير 2017

هذا المشروع البحثي سيقوم بدراسة وتمحيص تحدّيات عديدة تواجهها الصناعة النفطية في المجال المتعلّق بتماسك وموثوقية الهيكل الداخلي للآبار النفطية ، معدل وتسارع التآكل وخسارة المعدن للأنابيب والمواسير الحديدية المتعدّدة والمبطّنة لجدران الآبار المنتجة للنفط والغاز. وسيعتمد تقييم هذه التحديات على معلومات حقلية بناءا على أحدث التقنيات المستخدمة وهي سجلات الآبار عن طريق الموجات الكهرومغناطيسية.

سيقوم البحث بتطوير حلول هندسية وطرق معالجة مبتكرة و مبنية على تقدير المخاطر لحساب احتمالية فشل الأنابيب و المواسير الحديدية المتعدّدة والمبطّنة لجدران الآبار، وكذلك تطوير نماذج للتنبؤ بمدى درجات التآكل للمبادرة بمعالجته.

هذه الحلول ستسهم بدرجة عالية ومهمّة في تحسين مستويات السّلامة للأفراد والمنشآت النفطية ، والحؤول بدرجة كبيرة عن فشل وانهيار الآبار بسبب مشاكل التآكل، وكذلك تحسين اقتصاديات العمليات التشغيلية في الحقول النفطية.

سيكون ذلك متاحاً بناء على تطبيق نظام متابعة ومراقبة للآبار ذات المشاكل يأخذ بالإعتبار النتائج اللتي سيتوصل لها المشروع والذي يعتمد على معلومات حقلية موسّعة ممّا يزيد على خمسمائة (500) عيّنة دراسية من حقول نفطية سعودية.

سيقوم البحث بمراجعة شاملة ومستفيضة لكافة الجوانب المتعلقة بتماسك هيكل الآبار والتقنيات المستخدمة لقياس ومراقبة مشاكل التآكل وكيف تطوّرت هذه التقنيات واستخدمت لتؤثر على استراتيجيات التشغيل في الحقول النفطية وخصوصاً ماكان منها في المراحل المتأخرة من دورة الإنتاج.

CHAPTER 1

INTRODUCTION

Saudi Arabia has one of the largest and most mature oil and gas fields. Therefore, shifting the paradigm of well integrity surveillance practices from reactive to proactive through capitalizing on the best-in-class technology and research capabilities will have an enormous impact on the sustainability of such invaluable assets.

Sound well integrity management strategy in mature fields where wells can sustain economic production for thirty to fifty years is vitally important. Failing to achieve this strategy would cause catastrophic loss in both assets and human beings. Surface leaks are one example, not to mention the huge cost to be afforded. These leaks are caused by downhole multiple casings impairment due to active shallow aquifers corrosion.

Downhole corrosion is the main threat to the integrity and upkeep of wellbore completion tubulars. It is categorized into internal corrosion and external corrosion. Internal corrosion is mostly caused by production/injection fluids. It attacks the inner downhole tubing or casing depending on the completion type. Whereas, external corrosion attacks the outer downhole casings and can cause dramatic loss of assets and production. Water-bearing formations especially at shallow depths are the main source of external corrosion. Poor cement bond behind casings promotes and accelerates external corrosion growth. This is mostly observed across loss-circulation zones where cement quality is questionable.

Casing integrity surveillance program consists primarily of temperature and annuli surveys. One common aspect among these surveillance tools is the detection of casing failures after their occurrence. Corrosion logging, another surveillance tool, provides the most direct measurement of casing integrity and can be used as a predictive measure as well. Mechanical, ultrasonic, and electromagnetic tools are three main types of corrosion logs. The latter type will be thoroughly discussed in the proposed research work.

1.1 Well Integrity

1.1.1 Brief Background

Well Integrity is defined in NORSOK D-010 as the "application of technical, operational and organizational solutions to reduce risk of uncontrolled release of formation fluids throughout the life cycle of a well". NORSOK stands for "Norsk Sokkels Konkurranseposisjon" (the competitive position of the Norwegian continental shelf) [1]. NORSOK standards are developed by the Norwegian petroleum industry to ensure adequate safety, value adding and cost effectiveness for petroleum industry developments and operations[1]. Historical rates of well "failure" in oil and gas fields vary from a few percent of wells with barrier failures to more than 40%[17]. Analyses of 8,000 offshore wells in the Gulf of Mexico shows that 11–12% of wells developed pressure in the outer strings (called "sustained casing pressure"), as did 3.9% of 316,000 wells in Alberta[17] [34] . Considine et al. used state violation records to estimate that 2.6% of 3,533 gas wells drilled between 2008 and 2011 had barrier or integrity failure. Vidic et al. extended the timeline (2008–2013) and number of wells studied (6,466) and found that 3.4% had well-barrier leakage, primarily from casing and cementing problems. Davies et al. estimated that 6.3% of wells drilled between 2005 and 2013 had a well-barrier or integrity failure, consistent with Ingraffea et al.'s number of 6.2% for unconventional wells.

1.1.2 Consequences of Well Integrity Loss

History shows some severe examples of losing integrity in wells such as the Phillips Petroleum's Bravo blowout in 1977, Saga Petroleum's underground blowout in 1989, Statoil's blowout on Snorre in 2004, and BP's Macondo blowout in the Gulf of Mexico in 2010. These serious accidents remind us of the potential dangers in the oil and gas industry and they are some of the main drivers for the current focus on well integrity in the industry[31]**.**

1.1.3 Well Integrity Surveillance

Well integrity surveillance is an essential part of any well integrity management strategy aimed at maintaining the healthiness of all completion components. Surveillance tools are divided into two main categories depending on their specific application and use:

- Reactive tools such as temperature and annuli surveys that can detect downhole leaks after their occurrence.
- Proactive tools such as corrosion logging technology that can predict eminent leaks before their occurrence and quantify the integrity of single or multiple downhole tubulars.

Temperature Surveys are used for early detection of casing leaks and/or fluid movements behind pipe which can result in contamination of aquifers, loss of oil production or even surface blow-outs. Whichever occurs will affect the character of the temperature gradient recorded for that particular well. Timely identification of casing leaks is critical to avoid the loss of hydrocarbons and contamination of shallow aquifers. A subsurface temperature profile normally shows an increase in temperature with depth from ambient or surface temperature to reservoir temperature. In classical examples, the gradient is a straight line with a slope of about 1.5 degree Fahrenheit per hundred feet of depth[26]. Under field conditions, this linearity is distorted due to natural differences in thermal conductivity among zones, fluid movements within the zones and effect of wellbore deviation. **Figure-1** below portrays the temperature profile anomalies when a cross upward or downward flow takes place.

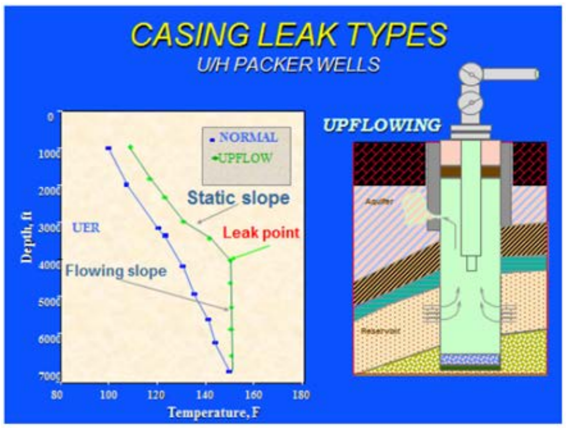

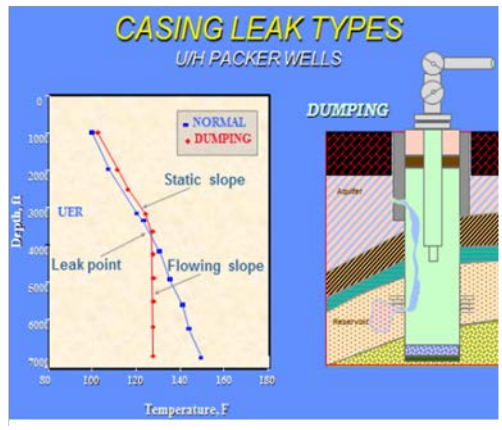

Figure 1: Example of temperature profile anomalies when a cross upward or downward flow takes place (after Saudi Aramco Well Integrity Surveillance Manual, 2012).

Annuli Survey is a technical term describing the measurements of annuli pressures in a frequent basis. Annulus is any space between pipes, tubing or casing and the formation surrounding it[26]. It is named after the corresponding geometric concept. During the drilling process, the presence of an annulus gives the ability to circulate fluids in the well. In a completed well, there may be different annuli. The "TCA" annulus is the space between the production tubing and the production casing string. The TCA annulus can serve a number of crucial tasks, including gas lift and well kills. A normal well will also have a "CCA-1" and frequently a "CCA-2" annulus or more, between the different casing strings as shown in **Figure-2** below. These annuli do not normally have any connection to the wellbore fluids, but maintaining pressure in them is important in order to ensure the integrity of casing strings. Analyzing trends of annuli surveys and integrating the data together is essential to troubleshoot any suspected problem. An increase or decrease in annuli pressures and any change in the trend behavior should be treated as a suspected problem until proven otherwise.

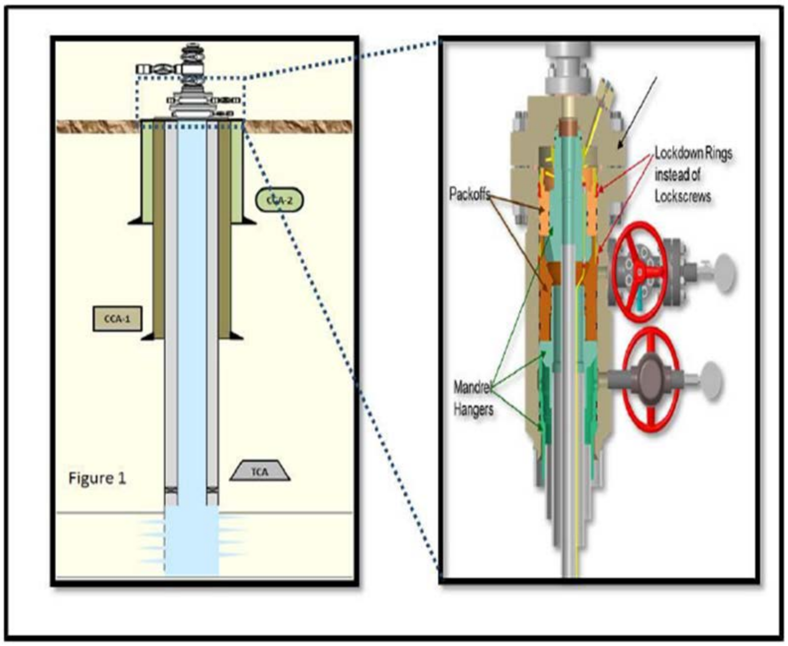

Figure 2: Illustration of different annuli in a well (after Saudi Aramco Well Integrity Surveillance Manual, 2012).

1.2 Wellbore Corrosion

1.2.1 Definition

Corrosion in its simplest definition is the loss of electrons from a metal causing the metal to transform to its ionic form and hence corrode. The term corrosion is sometimes also applied to the degradation of plastics, concrete and wood, but generally refers to metals[2]. Corrosion occurs because metals tend to revert to more stable forms in which they are found in nature initially, i.e., oxides, sulfates or carbonates. Corrosion is defined by the American

Electrochemical Society as the destruction of a metal by chemical or electrochemical reaction with its environment[14]. The destruction of metals by corrosion occurs by:

- Direct chemical attack at elevated temperatures in a dry environment.
- Electrochemical process at lower temperatures in water-wet or moist environment.

1.2.2 Principles

Oxidation takes place when a given substance loses electrons and reduction occurs when there is a gain in electrons. A substance that gives electrons is called reducing agent, whereas the substance that gains electrons is called oxidizing agent. Electrons are always transferred from the reducing agent (anode) to the oxidizing agent (cathode). Within the process, the corrosion products are formed as:

- Ions in solution, removed from the metal surface.
- Ions precipitated as various salts on metal surfaces.
- Released Hydrogen gas or Hydrogen evolution.

The basic electrochemical reactions, which occur simultaneously at the cathode and the anode cause many forms of corrosion **(Figure-3)**. At the cathode, the hydrogen or acid ion removes electrons from the cathodic surface to form hydrogen gas. At the anode, a metal ion is released due to the loss of the bonding electrons and passes into solution or reacts with another component to form scale. Dissimilar metals exposed to electrolytes exhibit different potentials to go into solution or react with the environment. It is worth noting that when the reaction area of cathodes to that of anodes (C/A ratio) is high, the corrosion rate at anodes will be high as well.

In case of electrochemical reaction which is the main method of corrosion of metals in drilling and production operations, the magnitude of electrochemical potential for a particular metal determines the tendency of the reaction to proceed. Under ambient conditions, the oxidation of most metals is thermodynamically spontaneous, with the notable exception of gold and platinum[15]. Whereas the resistance offered by the corrosion products to the continued progress of the reaction determines the rate of corrosion. Electrochemistry is the principle drive behind the oxidation and reduction reactions. The ideology of electrochemistry as well as its most widely used terms are introduced and defined below:

- Electric potential (E) the capacity of an electric field to perform work, measured in volts.
- Electric current (I) the movement of electrically charged particles, measured in amperes.
- Resistance (R) determines the amount of current through the object for a given voltage across, measured in ohms.
- Electric charge is the quantity for electric charge in coulombs.
- Electrical energy is the energy made available by the flow of electric charge through an electrical conductor, measured in joule.

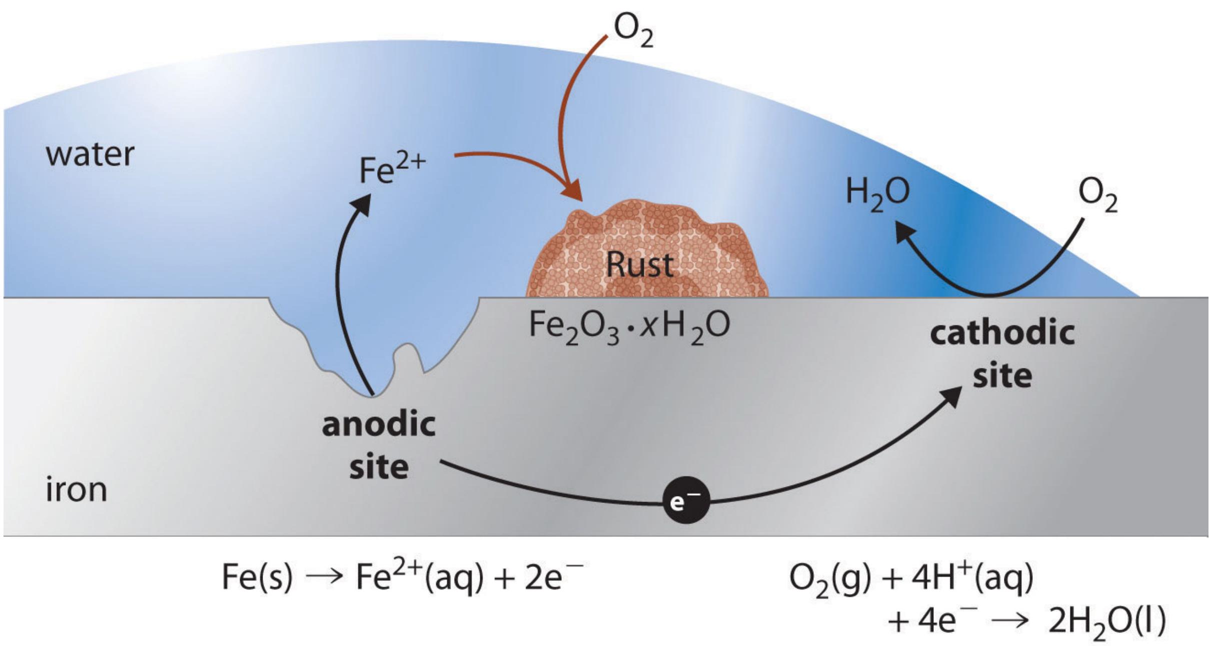

Figure 3 Typical Galvanic Cell (after http://2012books.lardbucket.org)

1.2.3 Conditions Promoting Corrosion Growth

Corrosion is a relentless process that never stops. As a matter of fact, the rate at which metal is lost is further accelerated in the presence of:

- A driving force or electrical potential.
- Saline water acting as an electrolyte.
- Anodic and cathodic sites.

In a wet environment, aqueous corrosion can occur due to electrochemical processes which depend upon metal ion transport and reaction[13]. Gradients of metallic and electrolytic ion concentrations, temperature, ambient pressure, and the presence of other metals, bacteria, or active cells, all influence the corrosion rate[13]. An external conductor is a must to complete the electrochemical reactions and hence corrosion circuit. Also, a rise in temperature (within a reasonable limit) increases the rate of corrosion[20].

The various components that are involved in the process of corrosion of metal are:

- The metal susceptible to corrosion.
- The films of hydrogen gas and metal corrosion products,
- The liquid and gaseous environment and
- The several interfaces between these components

The external casing corrosion may be caused by the presence of one or combination of the following:

- Presence of corrosive formation water (having high salinity)
- Presence of bacterially generated H2S
- Presence of electrical currents
- Presence of corrosive completion fluids

1.2.4 Corrosion Mechanisms

Various forms of corrosion may take place in the wellbore. Corrosion mechanism can be sub-divided into three categories:

- Electrochemical Corrosion
- Chemical Corrosion
- Mechanical Corrosion

Electrochemical corrosion involves exchange of current and formation of a cell-like system. This type of corrosion mainly occurs on the outer walls of the casing and is esponsible for many downhole leaks. This can be further subdivided into galvanic, crevice, pitting and Intergranular corrosion as[18]:

1. **Galvanic corrosion** occurs because of dissimilar metals and the presence of electrolyte. This is easily satisfied when difference in metals from joint to joint, joint to collar or within the joint itself exists[30].
2. **Crevice corrosion** occurs adjacent to casing section exposed to different fluids or when a casing is exposed to a fluid and the other is not. Both scenarios create an anode /cathode pair. This type of corrosion occurs mainly in poorly cemented casings[30].
3. **Pitting corrosion** which often creates holes in casings. This can be initiated by small scratches, defects and impurities in the casing metal.
4. **Intergrannular corrosion** is due to the presence of impurities such as oxides on the grain boundaries. The discontinuity in metal composition may stimulate small galvanic reactions when casing is exposed to saline corrosive fluids.

Chemical corrosion involves chemical reactions that may not produce appreciable voltages. Most of these mechanisms occur on the inner wall of casings[30].

Mechanical corrosion is caused by stresses in the casing such as unsupported casing, tubing set under tension or compression, high differential pressure across casing or damage to the casing wall during drilling operations[30].

Erosion corrosion is caused by fast moving fluids and solids that strip out the casing or tubing wall of its protective coating causing accelerated corrosion. If solids are present in the stream erosion can occur quickly.

1.3 Corrosion Logging Technology

In this section, major industry available corrosion logging tools, their applications, limitations and outputs are presented. There are three types of corrosion logging tools as follows:

1. Mechanical Tools such as the Multi-Finger Caliper Tool.
2. Ultrasonic Tools.
3. Electromagnetic Tools.

1.3.1 Multi-Finger Caliper Tool

This tool uses multiple high resolution calipers which measure slight changes in the internal diameter of tubing and casing strings[24]. The tool deploys an array of hard-surfaced fingers, which monitor the inner pipe wall. Each of the sensors generates an independent signal that is recorded versus depth. The tool is equipped with centralizers to ensure effective centering force in highly deviated intervals. The MFCT can detect casing deformation, bending, fractures, holes, scale deposition, paraffin build-up, and inner wall corrosion with high accuracy. The measurements are not affected by wellbore fluids. The resolution of the tool depends on the number of “feeler” arms mounted on the tool where the higher the number of calipers the higher the azimuthal resolution. The main limitation of the tool is the inability to detect external corrosion as it can measure the inside diameter only.

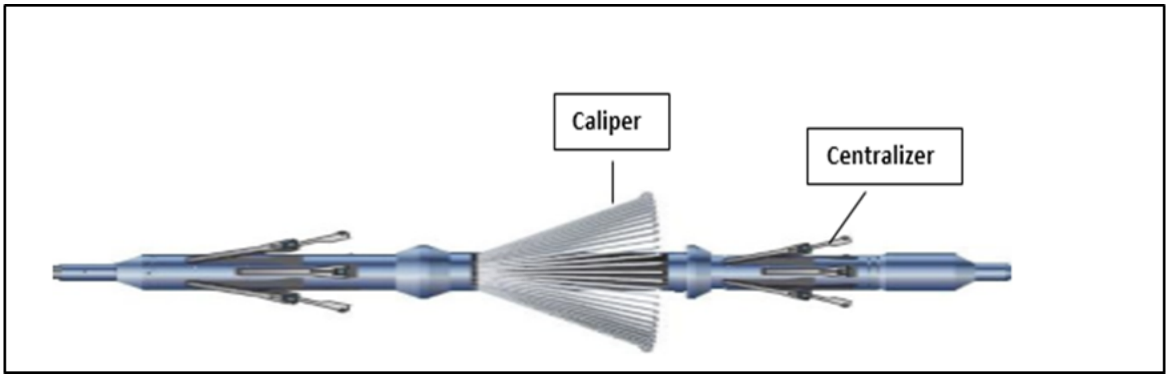

Figure 4: Multi-Finger Caliper Tool (after Saudi Aramco Well Integrity Surveillance Manual).

1.3.2 Ultrasonic Tool

This tool uses a rotating ultrasonic transducer to measure the echo transit time and the signal strength of the ultrasonic pulse. The low frequency (200-700 Hz) ultrasonic pulses travel through the well fluids and reflect off the casing wall, resonating the casing in the thickness mode[30]. Signal arrivals are then analyzed to provide the casing thickness and surface condition images reflected from the internal and external casing interfaces. Precise radius and thickness measurements enable quantifying the depth of an anomaly. Low frequency tools provide the resolution and sensitivity needed to measure pits and other anomalies down to diameters as small as 1.2 inch on either the inside or outside surface. High frequency ultrasonic tools provide the resolution and sensitivity needed to measure pits and other anomalies down to diameters as small as 0.3in either on the inside or outside surface. This tool makes absolute measurements so that corrosion and other casing anomalies can be identified and measured without reference to a base log. The tool is most applicable in cases where good azimuthal coverage of the pipe is required or where corrosion on the outside surface of the casing is suspected.

The ultrasonic interpretation is sensitive to the acoustic properties of the fluids. The tool cannot be run in gas wells as the fluid density is below the minimum allowable limit. Killing operation is required before running USIT to displace the wellbore with liquid that has a density below the maximum limit. In addition, excessively corroded pipe or scale may distort the pulsed echo signals and affect the interpretation.

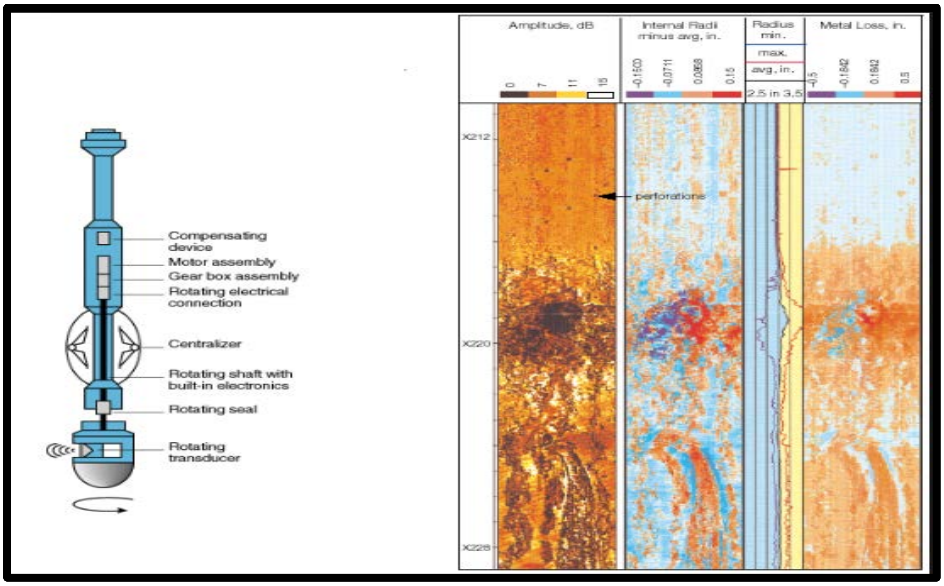

Figure 5: Ultrasonic Tool (after Szary, T., 2006).

1.3.3 Electromagnetic Induction Tool (EMIT)

This tool primarily detects the average total metal loss of all available pipe strings[7]. The tool uses three types of non-invasive electromagnetic measurements to characterize well casings employing low, medium and high frequency induction currents which are related

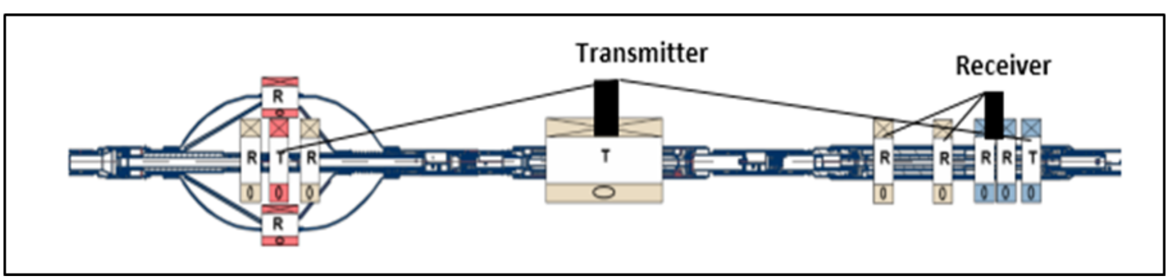

Figure 6: Electromagnetic Induction Tool.

to the casing wall thickness, inside diameter, and permeability or conductivity. The lower the frequency, the deeper the penetration is to the outer casings. Each parameter is averaged around the pipe circumference. The tool has multiple transmitters and receivers to send and receive the electromagnetic signals. It detects average metal loss and changes in casing geometry regardless of the fluid type.

Despite its ability to assess multiple casings metal loss, the tool can only read an azimuthal average loss across multiple strings. Consequently, wells with casing failures will definitely show average metal loss values less than 100% unless the failure occurs around the 360o circumference. In other words, 50% average metal loss could mean a failure if one part of the casing is completely gone and the other stays intact **(see Figure-7).**

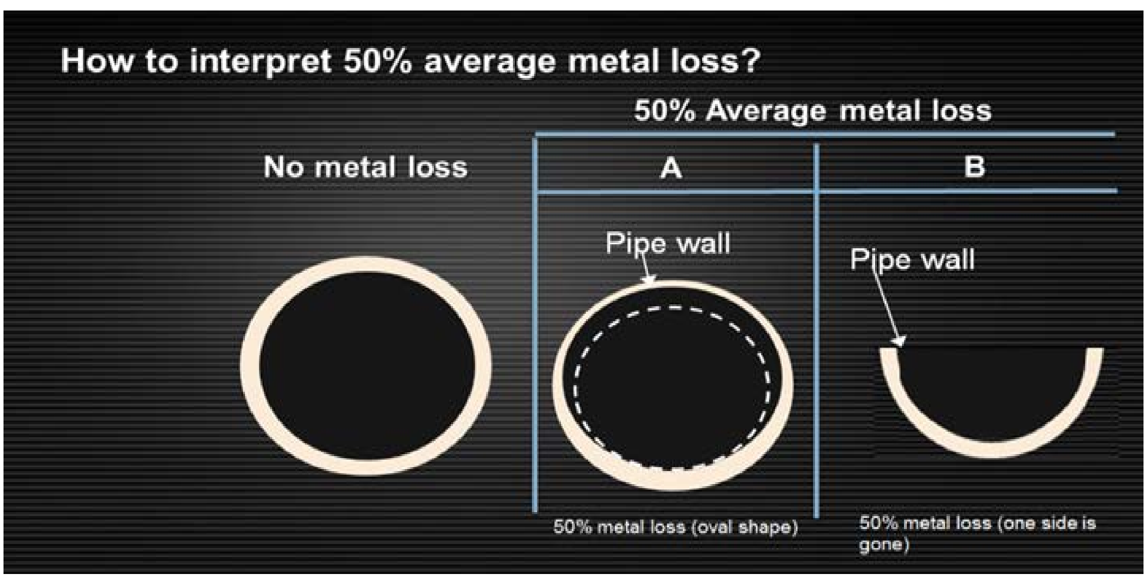

Figure 7: Different possibilities when the EMIT tool reads 50% metal loss on average. Case B is the worst-case scenario as it shows 100% metal loss on one side and 0% on the other.

1.3.4 Electromagnetic Defectoscope Tool (EMDS)

This tool has the same working principle as EMIT yet can provide the metal thickness of individual casings and tubing. The tool employs an electromagnetic transmitter and receiver coils to induce transient or pulsed eddy currents in the cross section of the tubulars being evaluated and measure the decaying electromagnetic response generated from the induced signal with the receiver coils[36]. When AC power is supplied to the emitting coil, an electromagnetic field is generated that creates an electrical current around the tubing and casings. This current induces a voltage on the receiving side of the coil that is related to the pipe average metal thickness loss (see **Figure-8**). EMDS tool has many different versions with different radii of investigation that can go up to 4 casings strings in tubing-less completions and 3 casings strings in tubing completions.

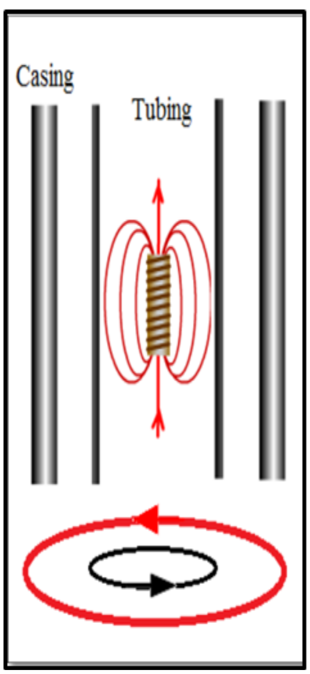

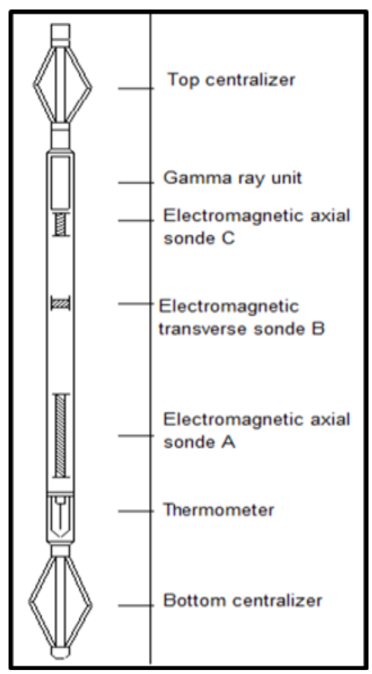

Figure 8: EMDS working principle (on the left) and tool's configuration (after Zhang, S., 2013).

EMDS tool has the same limitation when it comes to metal loss averaging. The special feature EMDS tool has over EMIT is the ability to determine the average metal loss of individual pipes. Depending on tool type, casings’ failures can be detected at average metal loss percentages as low as 15-20%. This has been verified by looking at the tool response across actual casing failures in multiple wells.

CHAPTER 2

LITERATURE SURVEY

(STANLEY et al, 1962) introduced a new Electromagnetic (EM) casing inspection tool to the industry. He described the existence of internal and external casing damage due to corrosion and other causes as a problem in many oil fields. The author stated a fact that prior to the development of the casing inspection tool, there has been no method by which to determine the extent of external casing damage. External damage usually became known when a casing leak developed. The author also described the theoretical basis of this new logging tool as a method of measuring the effect of eddy-currents on a magnetic field. The theory of eddy-currents indicates that the phase shift will be determined by four factors:

1. Casing wall thickness.
2. Frequency of alternating current.
3. Electrical permeability and resistivity of the metal.

The basic phase-shift equation which follows indicates that the phase shift will be proportional to casing-wall thickness.

$$\emptyset = 2\pi D\sqrt{\frac{F\mu}{\rho \times 10^3}} \tag{1}$$

Where,

∅: Phase shift.

D: Depth (cm).

***μ*:** Relative permeability.

***ρ*:** Resistivity (micro-ohm cm).

F: Frequency (cycles per second).

The author has concluded that the utilization of this new tool should furnish information on the extent and the rate of casing corrosion to aid in the evaluation of protective measures and the planning of remedial work.

(EDWARDS et al, 1964) reported field results obtained with EM corrosion-detecting tool. The author also explained the principles of operation, the types of equipment available for field use, interpretation principles as a result of laboratory and field experience, actual field results in various areas and recommended operating procedures. He concluded that although interpretation, techniques are not entirely quantitative, it is hoped that increasing field interpretation results will increase existing knowledge.

(Cuthbert et al, 1974) introduced the new Pipe Analysis Log that employs separate tests of the total casing wall and of the inner surface. Together, these two measurements permit detection, with a high degree of resolution, of small defects and corroded areas in the pipe, and also provide the ability to discriminate between defects of the inner and outer walls of a single string of casing. The author states that using the data from the new log along with the older wall-thickness measurement enable detecting and locating severe corrosion or defects in the outer casing of double strings. Example logs of the new casing inspection tool, selected from an extensive test program and nine months of commercial application, were presented and comparisons are made of the results from the new tool with defects observed in the pipe when out of the well. The author concluded that the utilization of the

Pipe Analysis Log in conjunction with previously used inspection techniques, such as the Electromagnetic Thickness Tool, provides additional information and more complete answers about the condition of single or concentric casing strings.

(Smith, 1981) introduced the ETT-C corrosion logging technology which was developed for the in-situ inspection of well casing. The author described the limitation of a previous tool (ETT-A) as follows; electromagnetic techniques are used to measure casing wall thickness, apparent magnetic permeability, and inside diameter. Previous tools of this type made a single measurement which was dependent on both wall thickness and magnetic permeability. The single measurement technique did not allow the log analyst to differentiate between thickness changes and magnetic permeability variations. The ETT-C system monitors magnetic permeability to obtain an independent wall thickness measurement. The author concluded that ETT-C was developed to overcome the ETT-A limitation of casing permeability dependence. Multiple field examples have been presented to illustrate the new tool's capability.

(Sharshar et al, 1991) presented a review of a multi-well approach to the analysis of corrosion logging measurements across 50 wells in the Dukhan field. The objective of the study was to understand corrosion phenomena throughout the field and to determine the relationships between corrosion in different wells. The author has also presented a statistical approach to corrosion mapping at different horizons. The approach has enabled the delineation of corrosive areas in Dukhan field. A conclusion was made based on the examined cases that further work is needed to understand why the oil producers are less prone to outer wall corrosion than the injectors.

(Brill et al, 2011) presented a slim EM corrosion logging tool that enables the assessment of multiple casing strings without the removal of production tubing. This technology requires running an additional log to inspect the inner casing string.

(Burton et al, 2011) presented the results of surface tests conducted using EM eddy current tools to test the tool response across an array of engineering multiple casing failures. Another objective of the investigator's work was to obtain a correlation defining the metal loss threshold value beyond which sever defects are detected.

(Rourk et al, 2013) has introduced a new EM technology called pulsed eddy current log. This log is claimed by the author to have the capability of discerning individual strings' metal loss values. The author has limited his work to the theoretical basis of the technology.

(Garcia et al, 2013) presented a field application of the pulsed eddy current technology where several comparisons with ultrasonic tool response were made. The results of these comparisons showed a good match. The authors concluded with the need to enhance the tool capability to inspect more than two casing strings with quantitative and repeatable results.

(Yateem et al, 2013) performed a comprehensive evaluation of EM eddy current tool results on more than 80 wells. The objective of this study was to understand the tool's response across leaking and non-leaking hotspots confirmed during workover operations. The authors concluded that the uncertainty associated with EM eddy current tool was evident. Moreover, safe threshold of 50% average metal loss from the eddy current tool was set to classify the high risk of casings' failures. This threshold was based on the observations and data analysis of the subject case studies.

CHAPTER 3

PROPLEM STATEMENT

Electromagnetic corrosion logging tools are the best-in-class when it comes to multiple casings metal loss assessment. However, most of the data acquired are more of qualitative than quantitative measurements. This is attributed to the fact that electromagnetic tools provide circumferential average readings of metal thickness loss across multiple strings rather than directional ones. Consequently, wells with casing failures will definitely show average metal loss values less than 100% when logged with electromagnetic tools, unless the failure occurs around the 360^0 circumference. In other words, 50% average metal loss could mean a failure if one part of the casing is completely gone and the other part remains intact.

The problem statement of this research has three main parts as follows:

1. Quantifying the uncertainty associated with the averaging limitation of EMIT corrosion logging tools. This will be discussed in chapter five.
2. Formulating a risk based model to analyze EMIT corrosion logging data and assist preventive maintenance workover decisions with data-driven inputs. This will be discussed in chapter six.

3. Designing an EMIT corrosion logging frequency that takes into account the variation in corrosion rate over time. This will be discussed in chapter seven.

CHAPTER 4

EMIT CORROSION LOG ANALYSIS

The objective of this section is to define key modeling parameters and assumptions used for EMIT logs analysis.

4.1 Casing Integrity Assessment

Casing integrity is a fundamental part of any well integrity program. Casing integrity is about the mechanical integrity state of casing metal that prevents formation fluids from cross flowing into shallow aquifers or to surface and mechanically support the formations from deformation throughout the life of a well. It is therefore of a paramount for safeguarding wells, avoiding loss of valuable hydrocarbon resources and eliminating contamination of shallow aquifers. Casing integrity assessment may involve casing corrosion evaluation, casing mechanical strength estimate to tell how close each casing is to mechanical failures at given operating conditions such as pressure, temperature and produced fluid composition, if the casing is exposed to production.

4.2 Electromagnetic Corrosion Logs Analysis Assumptions

The presiding assumptions applied to interpret EMIT corrosion logs are listed below:

- The corrosion is assumed to be external considering the worst-case scenario at which casing strings are lost one by one and outside-in **(see Figure-9).** This assumption becomes more valid across known corrosive formations and loss circulation zones where cement quality is poor and external corrosion growth is expected. It is also more valid in wells completed with tubing and packer where the non-corrosive packer fluid inhibits internal corrosion growth.

- Unless there is a log for the inner tubing diameter, the production tubing is assumed to be in a perfect condition and total metal loss is taken from the outer casing strings considering the worst-case scenario.
- Unless there is a base log performed using the same tool, the average corrosion rate is calculated using the nominal thicknesses of the casing strings.
- In case the total nominal thickness is more than the maximum measurable thickness of the tool, then the results are deemed qualitative.

The above assumptions will form the bases for modeling the external corrosion growth in multiple casings and predicting the remaining completion life.

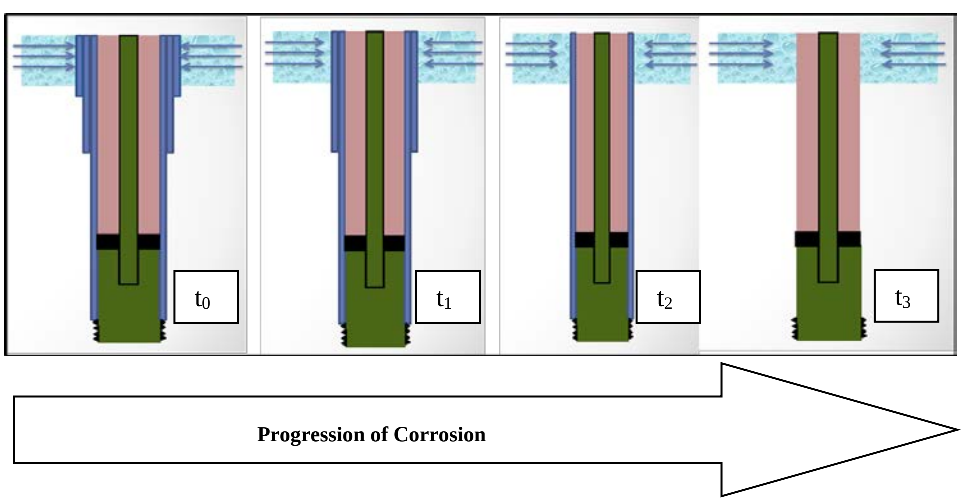

Figure 9: An illustration of the external corrosion concept.

4.3 Interpretation of EMIT Logs

Data to be interpreted in a typical EMIT corrosion log report are total remaining thickness and average metal loss percentage at all hotspots **(see Figure 10)**. The time it takes to reach the measured metal loss in multiple casings is also a key input during the data interpretation process. Key parameters derived from the raw logging data will be defined to quantify the wellbore integrity. These parameters should address the following:

- Averaging issue of EMIT corrosion logging tool
- Completion type
- Number of casing strings
- Nominal thicknesses of casing strings
- Different combinations of casing strings
- Well age
- Workover interventions throughout the life of the well

Corrosion Summary

- Electromagnetic Casing Inspection Tool (EMIT-B) logged rigless 26-Jun-13 from 6543-0ft
- Original well completion date 11-May-1968
- Completion Strings Summary:

String OD	Weight (ppf)	Shoe Depth (ft)	Nominal Thickness
13 3/8	61	2398	0.430
9 5/8	36	4378	0.352
7	23	6938	0.317
4 1/2	11.6	7389	0.250
2 7/8	6.4	6543	0.217

- Metal Loss Summary:

# of Strings	ML % Casings + Tubing	ML % Casings Only	Thickness of Hot Spot	Depth of Hot Spot
5	44%	51%	0.881	490ft
4	11%	14%	1.012	3946ft
3	10%	14%	0.703	6265ft
2	N/A	N/A	N/A	N/A
1	N/A	N/A	N/A	N/A

- Remarks:
  - 4-1/2in liner extended to surface from 6604ft
  - 1st 7in liner extended to 1969ft from 4176ft, and 2nd 7in liner extended to surface from 1969ft
  - EMIT identified 7in liners butting together at 1969ft and 4176ft
  - EMIT identified 4-1/2in tubing packer at 6400ft

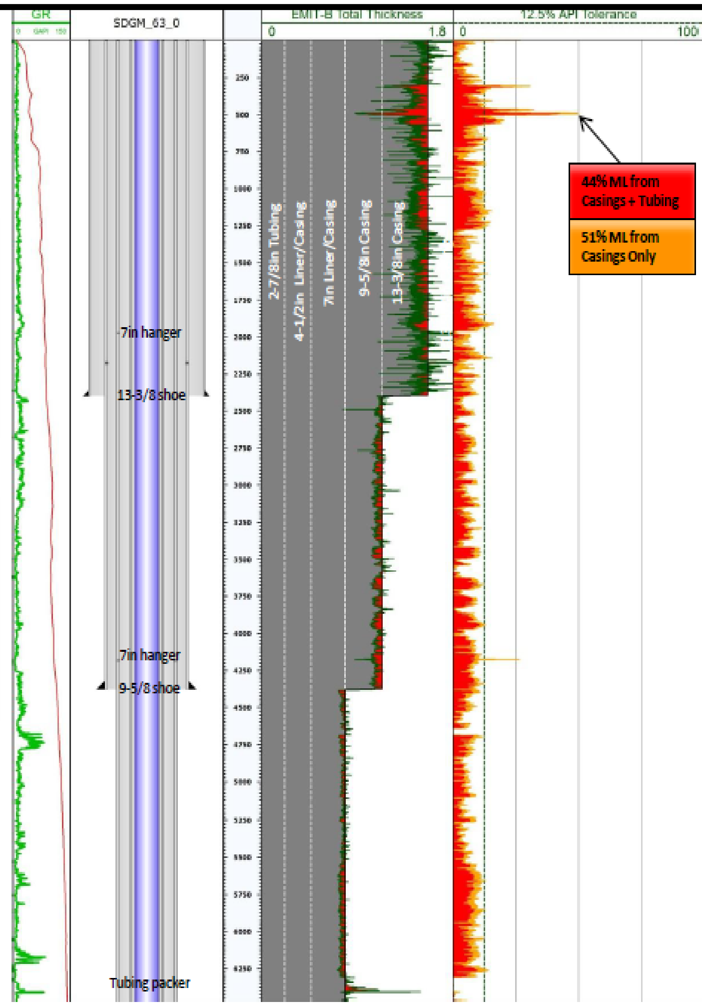

Figure 10: Example of EMIT report.

4.3.1 Average Remaining Barriers Ratio (ARBR)

EMIT provides the metal loss percentage out of the total nominal thickness as well as the remaining total thickness in inch. The metal loss breakdown per each string can be easily calculated taking into consideration the concept that casing strings are corroded externally one by one. The assumption of external corrosion growth is more valid in wells completed with tubing and packer where the tubing casing annulus is filled with inhibited brine or diesel preventing internal corrosion growth. Casing internal corrosion growth phenomenon may exist under specific conditions such as packer-less completions and mechanical casing damage during installation. The Average Remaining Barriers Ratio (ARBR) is the average number of remaining strings between the corrosive zones, usually water-bearing formations, and the wellbore divided by the number of nominal strings. It is a normalized parameter that accounts for different combinations and sizes of downhole casings.

The following formula is used to calculate ARBR:

$$ARBR \ = 1 - \frac{\left[\frac{T_{L1}}{T_{N1}} + \frac{T_{L2}}{T_{N2}} + \frac{T_{L3}}{T_{N3}} + \cdots \frac{T_{LX}}{T_{NX}}\right]}{X} \tag{2}$$

Where,

T_{L1}: Thickness loss from the outer string (in).
T_{L2}: Thickness loss from the second outer string (in).
T_{L3}: Thickness loss from the third outer string (in).
T_{N1}: Nominal thickness of the outer string (in).
T_{N2}: Nominal thickness of the second outer string (in).
T_{N3}: Nominal thickness of the third outer string (in).
X: Number of strings across the hotspot.

4.3.2 Corrosion Rate

Corrosion rate is quantified by different methods such as weight loss and rate of penetration. In our case, the latter method is applied to calculate the corrosion rate in mills per year using the below formula:

$$Corrosion\ Rate(mpy) = \frac{[Original\ Thickness(in) - Remaining\ Thickness\ (in)] \quad \times 1000}{Number\ of\ years\ since\ the\ last\ log} \tag{3}$$

For base logs, the original thickness will be the nominal one and the number of years will be the well age.

4.3.3 Expected Life:

Expected life of multiple/single casing string(s) is defined as the number of years before the average remaining thickness reaches a predefined retirement value. The formula to calculate expected casing life is as follows:

$$Expected\ Remaining\ Life(years) =$$

$$\frac{[Current\ remaining\ thickness(in) - Retirment\ thickness\ (in)] \times 1000}{Corrosion\ rate\ (mpy)} \quad (4)$$

Determining the retirement remaining thickness will be discussed in chapter six and seven.

4.4 Example Calculation of EMIT Log

In this section, an example of EMIT key parameters calculation will be presented. The objective of this is to further illustrate the tool's interpretation, demonstrate the ARBR concept and lay the ground for subsequent modeling of these parameters. Below are the steps to interpret a typical EMIT log of Well-A.

1. Two hotspots with the same average metal loss percentage were identified from the logging report as follows:
    a. 40% metal loss of triple casing.
    b. 40% metal loss of double casing.
2. Starting with the first hotspot, the total nominal thickness is given by 1.142 inch which is the sum of all nominal thicknesses of the three casing strings across this hotspot.
3. The total average thickness loss in inch for the first hotspot is calculated as follows:

$$Total\ metal\ loss(in) = Total\ original\ thickness \times Average\ Metal\ loss\ percent$$

$$= 1.142 \times 0.40 = 0.4568\ in$$

4. Assuming outside-in corrosion, the total metal loss is determined for each string starting from the outer casing all the way to the inner casing one after the other.

Casing String	Nominal Thickness (in)	Thickness Loss (in)	Total Number of Casing Strings (X)
1^{st} outer string (OD is 13-3/8 inch	0.430	0.430	3
2^{nd} outer string (OD is 9-5/8 inch)	0.395	0.0268	
Inner string or third outer string (OD is 7 inch)	0.317	0	
Total	1.142	0.4568	

Table 1: Example 1 for Metal Loss Summary of Each Casing String

5. The Average Remaining Barriers Ratio (ARBR) is calculated as follows:

$$ARBR = 1 - \frac{\left[\frac{0.43}{0.43} + \frac{0.0268}{0.395} + \frac{0}{0.317}\right]}{3} = 0.6440$$

6. As for the second hotspot, the total nominal thickness is given by 0.825 inch which is the sum of all nominal thicknesses of the two casing strings across this hotspot.
7. The total average thickness loss in inch for the second hotspot is calculated as follows:

$$Total\ metal\ loss(in) = Total\ original\ thickness \times Average\ Metal\ loss\ percent$$

$$= 0.825 \times 0.40 = 0.33\ in$$

8. Assuming outside-in corrosion, the total metal loss is determined for each string starting from the outer casing all the way to the inner casing one after the other.

Casing String	Nominal Thickness (in)	Thickness Loss (in)	Total Number of Casing Strings (X)
1st outer string (OD is 13-3/8 inch	0.430	0.33	2
2nd outer string or inner (OD is 9-5/8 inch)	0.395	0	
Total	0.825	0.33	

Table 2: Example 2 for Metal Loss Summary of Each Casing String

9. The Average Remaining Barriers Ratio (ARBR) is calculated as follows:

$$ARBR = 1 - \frac{\left[\frac{0.33}{0.43} + \frac{0}{0.395}\right]}{2} = 0.616$$

It can be noticed from the above example that at the same average metal loss percentage, the ARBR value of the two-string hotspot is less than the ARBR value of the three-string hotspot. This is due to the fact that ARBR parameter accounts for the number of remaining strings rather than the total remaining thickness.

CHAPTER 5

UNCERTINITY QUANTIFICATION OF EMIT CORROSION LOGS DATA

This chapter will focus on quantifying the uncertainty associated with EMIT average metal loss measurements. The chapter will also describe statistical methods of data collection and analysis used to quantify this uncertainty. Brief descriptions of basic statistical terminologies will precede the related chapter's topics for introduction.

5.1 Statistical Terminologies

- **Statistics:** is the study of how to collect, organize, analyze, and interpret numerical information from data.
- ***Population:*** A collection of units being studied. Units can be people, places, objects, properties or many other things. Statistics is mostly concerned with estimating numerical properties (parameters) of an entire population from a random sample of units from the population. In this research, examples of population will be the total number of wells in a field and total number of casing failures over the lifecycle of a field.
- ***Sample:*** A sample is a collection of units from a population. In this research, examples of sample will be the EMIT average metal loss percentage data and the group of logged wells by EMIT in a given field.

- ***Sample Mean:*** The arithmetic mean of a random sample from a population.
- ***Sample Standard Deviation:*** The standard deviation of a set of numbers is the root mean square of the set of deviations between each element of the set and the mean of the set.
- ***Z statistic or Z score:*** A Z statistic is a test statistic that shows how many standard deviations a certain value X is away from the sample/population mean. The equation used to calculate this value is as follows:

$$\text{Zstatistic} = \frac{[\text{X value} - \text{Sample mean}]}{\text{Sample standard deviation}} \tag{5}$$

- ***Histogram:*** A histogram is a bar graph that shows how frequently data occur within certain ranges or intervals (bins). The height of each bar gives the frequency in the respective interval.
- ***Normal Probability Distribution:*** A theoretical frequency distribution for a set of variable data, usually represented by a bell-shaped curve symmetrical about the mean. For each set of normally distributed data, there is a corresponding normal probability distribution that is a function of the sample's mean and standard deviation.

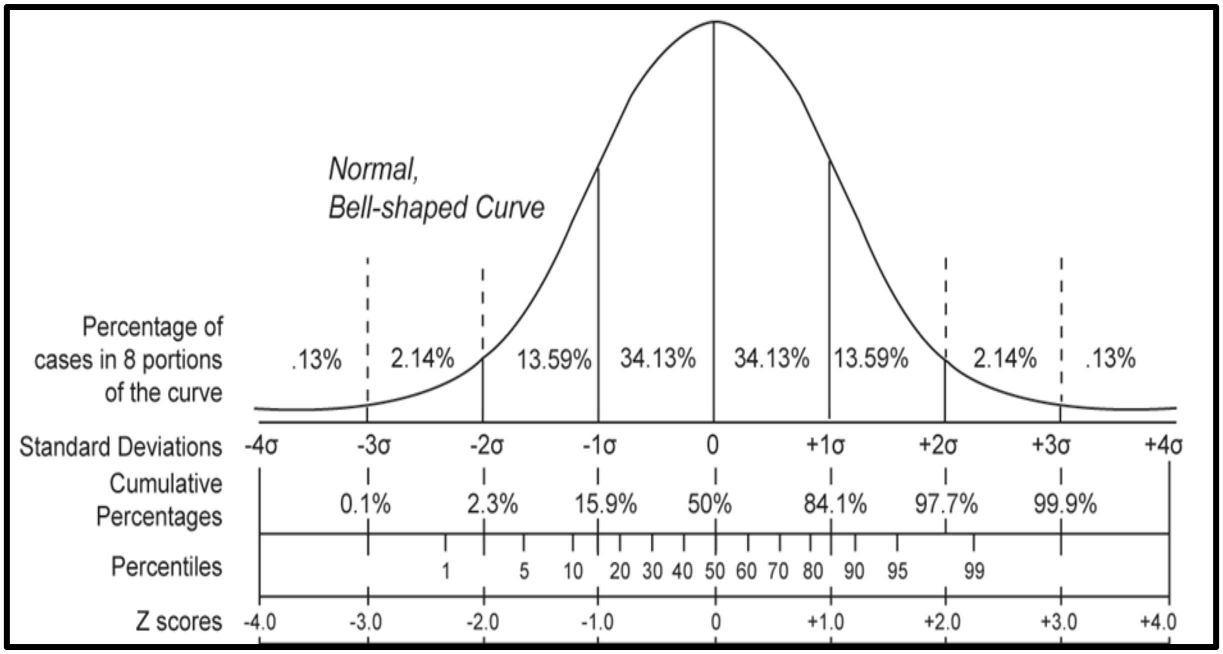

Figure 11: Normal Probability Distribution. Reprinted from Study.com, 2003.

5.2 The Data Set Under study

A cross-field data collection was conducted to assess the variation of EMIT response across known leaking and non-leaking average metal loss hotspots. In this research, two defined parameters will be used in relation to the assessment of casing corrosion; these are leaking and non-leaking hotspots. ***A leaking average metal loss hotspot*** is defined as the one measured by EMIT across confirmed multiple casings' leaks or failures. Casing failures are confirmed by different well integrity diagnostic methods, some of which are rigless such as annuli and temperature surveys and some are performed during rig intervention such as positive and negative pressure tests. On the other hand, ***a non-leaking average metal loss hotspot*** is the opposite where the EMIT measurements are taken across confirmed healthy multiple casings' conditions.

The total number of data points collected is **535 hotspots** from **218 wells**; out of which 498 are non-leaking and 37 are leaking average metal loss hotspots. A practical definition of a hotspot is any depth interval exceeding 12% average metal loss measured by the EMIT tool. This average metal loss tolerance was established by logging EMIT in four newly drilled wells to calibrate the tool's response across brand new casing strings.

The data set includes oil and water wells with different completion types and casings' grades, sizes and combinations. Well age is ranging between 2 to 67 years and the average metal loss hotspots were measured across a wide range of depths between 9 to 7723 feet. The below table presents the descriptive statistics of well age, hotspot depth and average metal loss values for both leaking and non-leaking data sets.

Parameter	**Leaking Hotspots**			**Non-Leaking Hotspots**		
	Average	Minimum	Maximum	Average	Minimum	Maximum
Well Age (years)	39.4	18	64	36.4	2	67
Hotspot Depth (ft)	1867	114	6116	3011	9	7723
Average Metal Loss %	62	40	82	27	1	74

Table 3: Summary Statistics of Leaking and Non-leaking Hotspots Key Parameters

It is clearly shown from the above table that the leaking and non-leaking key parameters overlap greatly leaving a wide range of undiscernible hotspots. For example, the overlap range in well age between the two data sets (leaking and non-leaking) is between 18 to 64 years which means that any hotspot well age within this interval can be either leaking or non-leaking. Similar conclusions are made about the two other parameters to emphasize on the uncertainty associated with casing leak prediction. In the next section, a methodical statistical investigation of the average metal loss parameter is presented to quantify this uncertainty.

5.3 Average Metal Loss Percentage Uncertainty

EMIT average metal loss measurements are subject to interpretation uncertainty. The fact that EMIT doesn't provide directional metal loss readings presents a challenge to define an average metal loss cutoff beyond which a preventive maintenance workover decision is made proactively before the well casings fail. Chapter one describes this challenge in great detail. The first step towards solving this challenge is to quantify the uncertainty using well known statistical methods. In this research work, a fundamental assumption is made that both leaking and non-leaking average metal loss data are normally distributed. Normality tests were performed on both data sets to validate this assumption. The normality test is a plot of the data ranked in an ascending order versus their percentiles on a normal probability scale. A straight line trend of the plotted data is the condition upon which the data set is classified as normally distributed. **Figures 12 and 13** below present the test results.

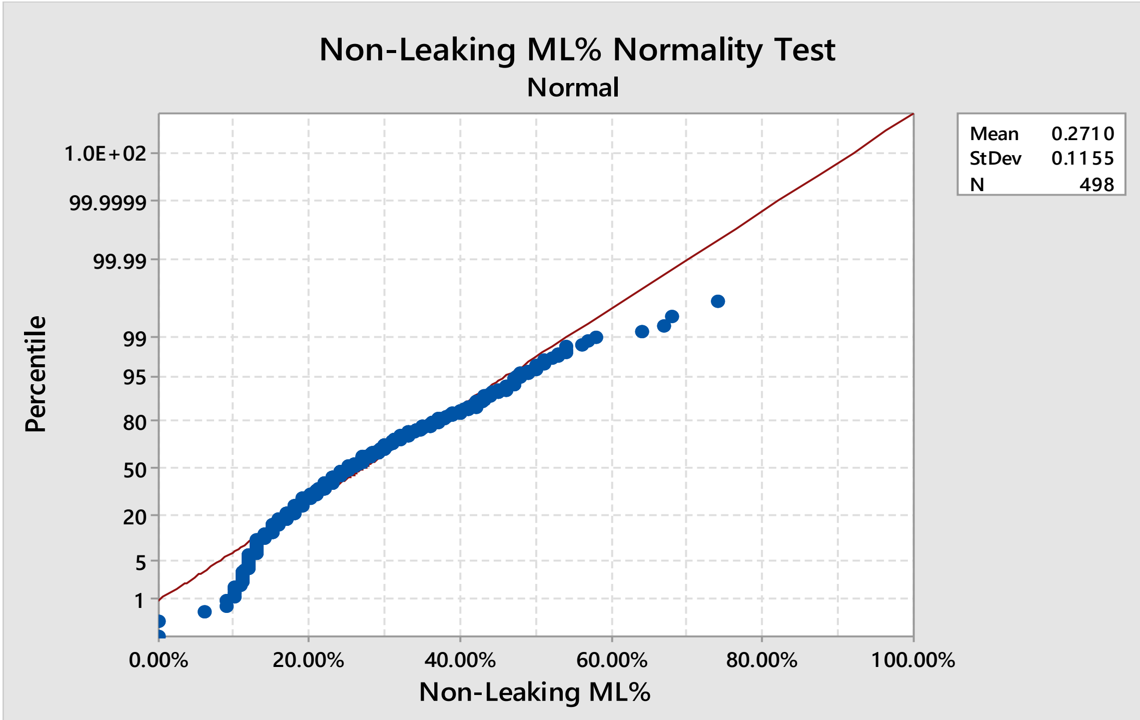

Figure 12: Leaking Average Metal Loss Data Normality Test.

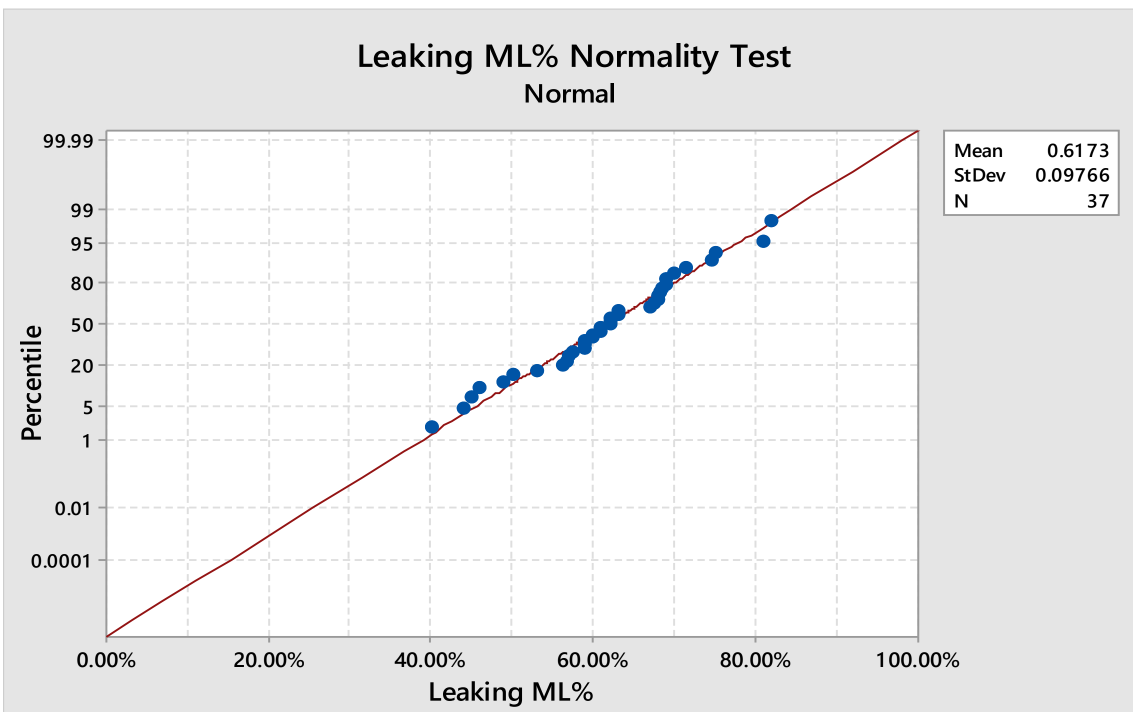

Figure 13: Non-Leaking Average Metal Loss Data Normality Test.

It can be clearly seen that both plots characterize the two data sets (leaking and non-leaking) as normally distributed. Generally, leaking hotspots data correlate more linearly on a normal probability scale than non-leaking hotspots data. This becomes more evident below 10% and above 60% average metal loss values on the non-leaking normality test plot **(Figure-13)**. In statistical terms, these data may be classified as outliers but not necessarily erroneous.

After identifying the distribution of both data sets, their probability density functions (PDFs) can be written in a mathematical form to generate their Normal Probability Distribution curves. These curves are plotted to relate the PDF versus average metal loss for both leaking and non-leaking hotspots. The steps followed to generate the PDF curves are as follows:

1. The **non-leaking hotspots** average metal loss values mean and standard deviation are calculated using the below equations:

$$\mu_{NLML} = \frac{\sum_{i=1}^{n}(NLML\%)i}{n} \tag{6}$$

$$\alpha_{NLML} = \sqrt{\frac{\sum_{i=1}^{n}(NLMLi - \mu_{NLML})^2}{n-1}} \tag{7}$$

Where,
$\boldsymbol{\alpha_{NLML}}$**:** Non-Leaking Metal Loss standard deviation (%).
$\boldsymbol{\mu_{NLML}}$**:** Non-Leaking Metal Loss mean (%).
NLML: Non-Leaking Metal Loss.

2. The **leaking hotspots** average metal loss values mean and standard deviation are calculated using the below equations:

$$\mu_{LML} = \frac{\sum_{i=1}^{n}(LML\%)i}{n} \tag{8}$$

$$\alpha_{LML} = \sqrt{\frac{\sum_{i=1}^{n}(LMLi - \mu_{LML})^2}{n-1}} \tag{9}$$

Where,

$\boldsymbol{\alpha_{LML}}$**:** Leaking Metal Loss standard deviation (%).

$\boldsymbol{\mu_{LML}}$**:** Leaking Metal Loss mean (%).

LML: Leaking Metal Loss.

3. The PDFs of both **non-leaking** and **leaking** hotspots are calculated as follows:

$$P_{NLML}(NLML) = \frac{1}{\sqrt{2\pi}\alpha_{NLML}}\ e^{-\frac{(NLML-\mu_{NLML})^2}{2\alpha_{NLML}{}^2}} \tag{10}$$

$$P_{LML}(LML) = \frac{1}{\sqrt{2\pi}\alpha_{LML}}\ e^{-\frac{(LML-\mu_{LML})^2}{2\alpha_{LML}{}^2}} \tag{11}$$

Where,

$\boldsymbol{P_{LML}(ML)}$**:** Leaking Metal Loss Probability Density Function.

$\boldsymbol{P_{NLML}(ML)}$**:** Non-Leaking Metal Loss Probability Density Function.

Equations (10) and (11) are plotted versus average metal loss in **Figure-14** below.

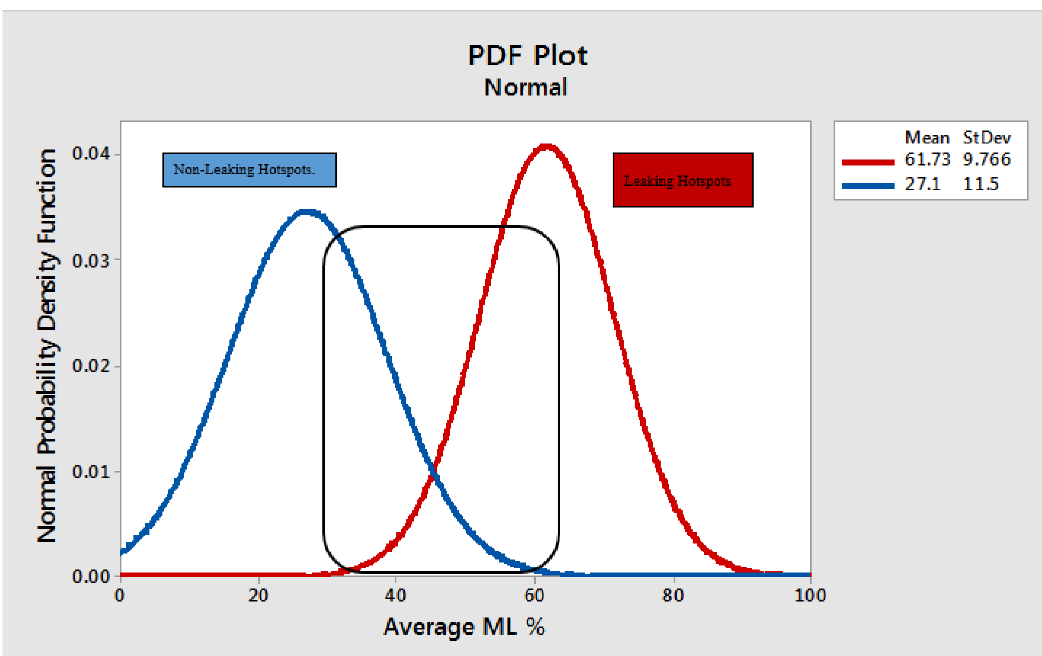

Figure 14: Metal loss leaking and non-leaking PDF plots.

Analyzing the above plots reveals and quantifies the uncertainty of EMIT average metal loss measurements. The average metal loss range delineated by the black box in **Figure-14** defines the interval within which a non-uniform external corrosion is likely to occur causing multiple casings failure (**scenarios A and B in Figure-7**). In fact, a casing leak is expected whenever we see an average metal loss value between 30% and 70%. Also, it can be inferred that the probability of a casing failure is 1 above 70% and 0 below 30% average metal loss.

5.4 Average Remaining Barriers Ratio Uncertainty

ARBR discussed in chapter four is a normalized mathematical transformation of the average metal loss parameter. The reason for introducing ARBR is that the metal loss value doesn't address the number of nominal casings, their thicknesses and combinations. For example, 50% average metal loss from 4 casing strings is less alarming than 50% loss from 2 strings. It is assumed in this research that EMIT response to average thickness loss in multiple casings is a strong function of these factors and not only the average metal loss percentage. Accordingly, the subsequent modeling of multiple casings failure will focus on ARBR as the statistical random variable of the probability distributions.

Similar to the pervious section, ARBR data will be categorized into **leaking** and **non-leaking data** sets. A normality test is also performed to decide whether the two data sets are normal or not. The below plots present the ARBR normality tests results.

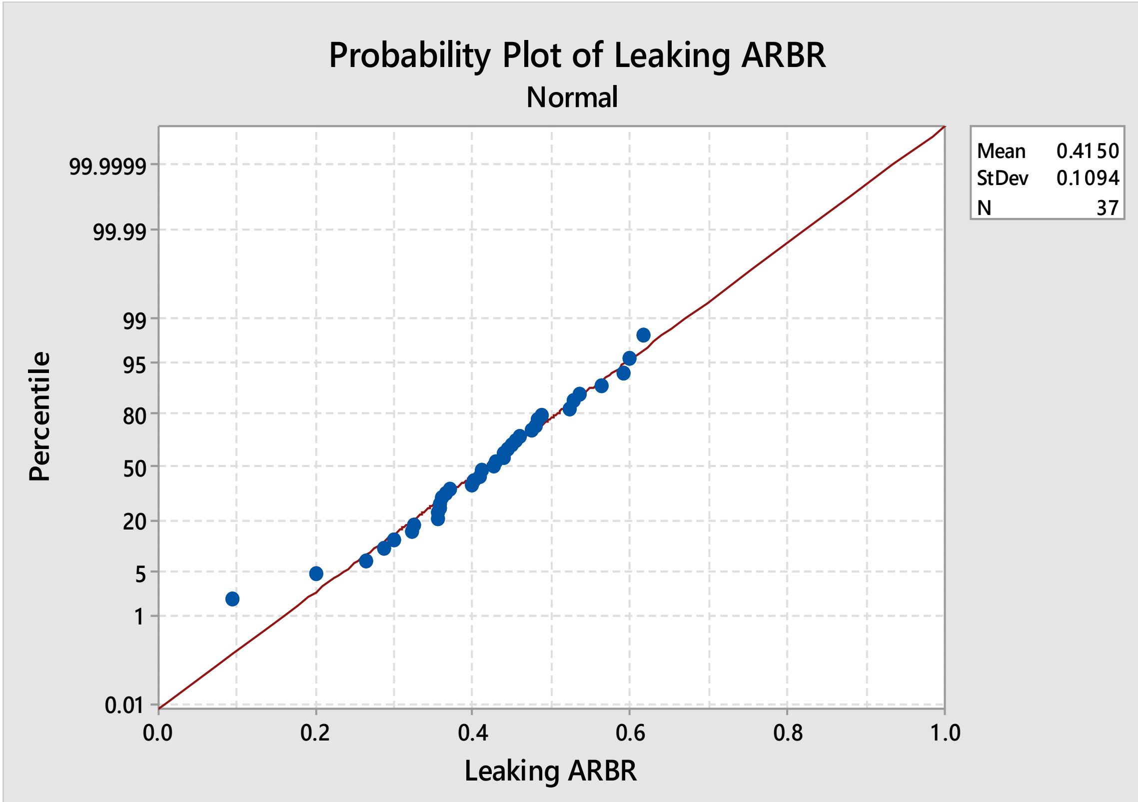

Figure 15: Leaking ARBR Normality Test.

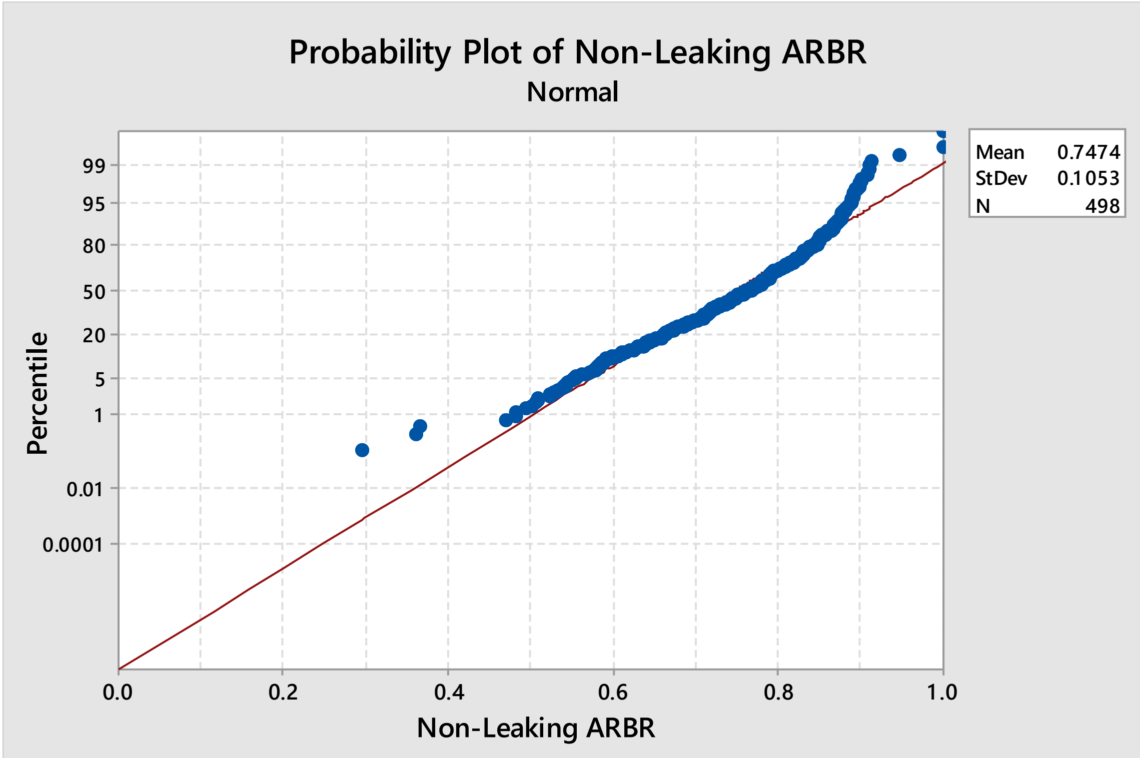

Figure 16: Non-Leaking ARBR Normality Test.

It can be clearly seen that both plots characterize the two ARBR data sets (leaking and non-leaking) as normally distributed. Generally and similar to the average metal loss data sets, leaking hotspots data correlate more linearly on a normal probability scale than non-leaking hotspots data. This becomes more evident below 0.3 and above 0.9 ARBR values on the non-leaking normality test plot **(Figure-16)**. In statistical terms, these data may be classified as outliers but not necessarily erroneous.

After identifying the distribution of both data sets, their probability density functions (PDFs) can be written in a mathematical form to generate their Normal Probability Distribution curves. These curves are plotted to relate the PDF versus ARBR for both leaking and non-leaking hotspots. The steps followed to generate ARBR PDF curves are as follows:

1. The **non-leaking hotspots** ARBR values mean and standard deviation are calculated using the below equations:

$$\mu_{NLARBR} = \frac{\sum_{i=1}^{n}(NLARBR)i}{n} \tag{12}$$

$$\alpha_{NLARBR} = \sqrt{\frac{\sum_{i=1}^{n}(NLARBRi - \mu_{NLARBR})^2}{n-1}} \tag{13}$$

Where,
$\boldsymbol{\alpha_{NLARBR}}$**:** Non-Leaking ARBR standard deviation.
$\boldsymbol{\mu_{NLARBR}}$**:** Non-Leaking ARBR mean.
NLARBR: Non-Leaking Average Remaining Barriers Ratio.

2. The **leaking hotspots** ARBR values mean and standard deviation are calculated using the below equations:

$$\mu_{LARBR} = \frac{\sum_{i=1}^{n}(LARBR)i}{n} \tag{14}$$

$$\alpha_{LARBR} = \sqrt{\frac{\sum_{i=1}^{n}(LARBRi - \mu_{LARBR})^2}{n-1}} \tag{15}$$

Where,
$\boldsymbol{\alpha_{LARBR}}$**:** Leaking ARBR standard deviation.
$\boldsymbol{\mu_{LARBR}}$**:** Leaking ARBR mean.
LARBR: Leaking Average Remaining Barriers Ratio.

3. The PDFs of both **non-leaking** and **leaking hotspots** are calculated as follows:

$$P_{NLARBR}(NLARBR) = \frac{1}{\sqrt{2\pi}\alpha_{NLARBR}}\, e^{-\frac{(NLARBR-\mu_{NLARBR})^2}{2\alpha_{NLARBR}{}^2}} \tag{16}$$

$$P_{LARBR}(LARBR) = \frac{1}{\sqrt{2\pi}\alpha_{LARBR}}\, e^{-\frac{(LARBR-\mu_{LARBR})^2}{2\alpha_{LARBR}{}^2}} \tag{17}$$

Where,

$\boldsymbol{P_{LARBR}(LARBR)}$**:** Leaking ARBR Probability Density Function.

$\boldsymbol{P_{NLARBR}(NLARBR)}$**:** Non-Leaking ARBR Probability Density Function.

Equations (16) and (17) are plotted versus ARBR in **Figure-17** below.

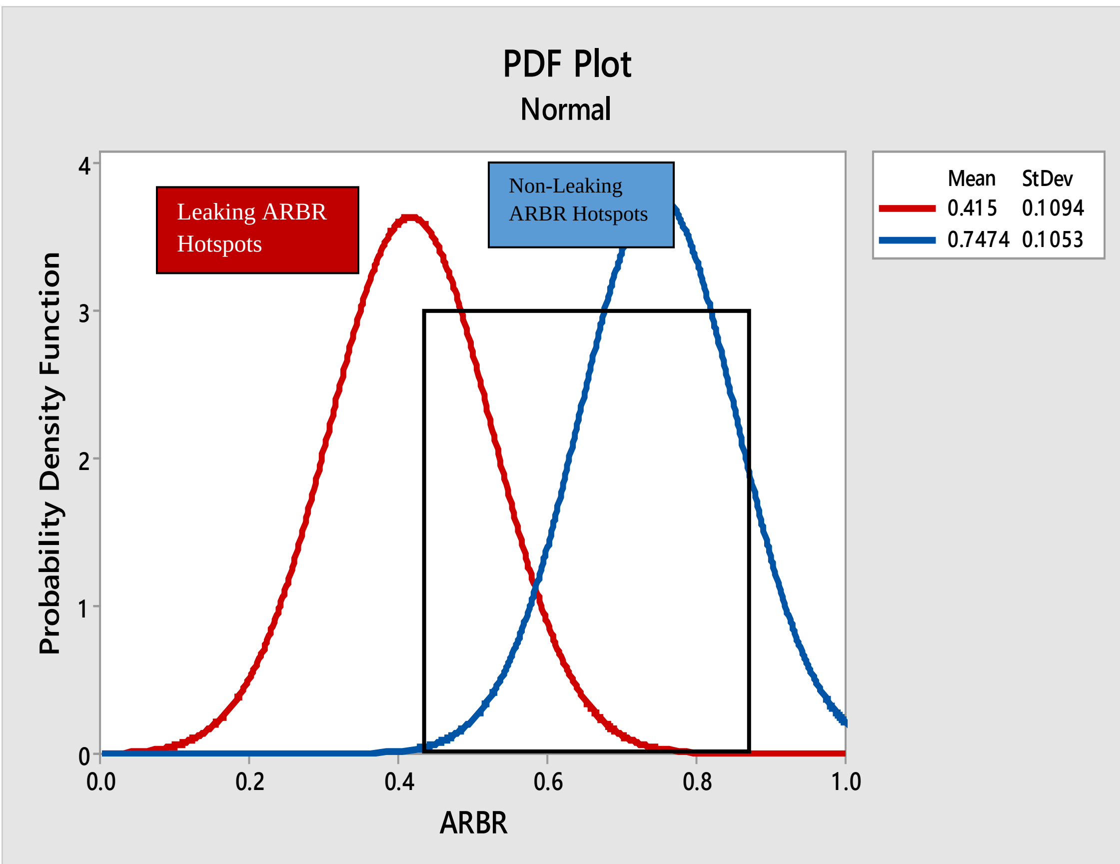

Figure 17: Leaking and Non-Leaking ARBR Normal Distribution Plots.

Similar to the average metal loss analysis, the above plots also reveal the uncertainty associated with ARBR. The ARBR range delineated by the black box in **Figure-17** defines the interval within which a non-uniform external corrosion is likely to occur causing multiple casings failure (**scenarios A and B in Figure-7**). In fact, a casing leak is expected whenever we see an ARBR between 0.4 and 0.8. Also, it can be inferred that the probability of a casing failure is 1 below 0.4 and 0 above 0.8 ARBR values.

CHAPTER 6

MODEL-ASSISTED DECISION MAKING

This chapter aims to achieve one essential goal of this research work; i.e. modeling the casing corrosion severity based on EMIT corrosion logs' data. Statistical models will be formulated to compute the likelihood of wellbore casings' failure taking into account the imbedded uncertainty due to the EMIT averaging problem discussed in chapters three and five. Overall, the expected milestones upon completing this chapter are to transform EMIT average metal loss data from qualitative responses of thickness reduction to actionable information in order to make prudent and cost-effective preventive maintenance workover decisions.

6.1 Casing Failure Concept and Probability

Casing integrity failure is an important concept to conceive before stepping into its mathematical modeling. In this section, we attempt to derive a probability of failure equation from ARBR leaking and non-leaking normal distributions. Key terminologies used in this derivation are defined below:

- **$ARBR_c$** is the cutoff value at and above which the probability of casing failure is computed.
- **$F_{hotspots}$** is the number of leaking/ failed hotspots at and above $ARBR_c$.
- **$SF_{hotspots}$** is the number of leaking/ failed hotspots below $ARBR_c$. The “SF” notion means that these hotspots survived from failure at and above $ARBR_c$ and then failed below it.
- **$SS_{hotspots}$** is the number of non-leaking hotspots below $ARBR_c$. The “SS” notion means that these hotspots survived from failure at and above $ARBR_c$ and still surviving below it.
- **L** is the total number of leaking hotspots.
- **NL** is the total number of non-leaking hotspots.

Figure-18 below is an illustration of these terminologies.

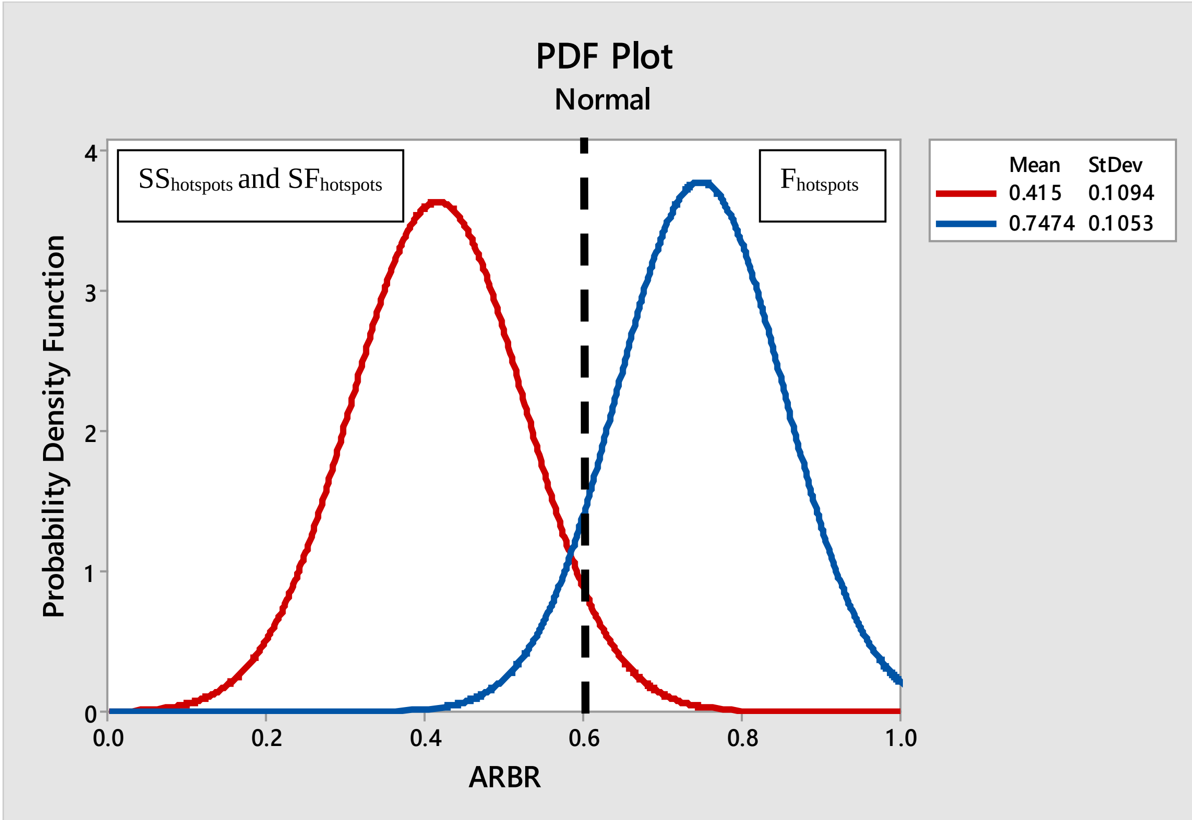

Figure 18: Illustration of casing failure probability derivation parameters.

The probability of failure equation will be derived in terms of $ARBR_c$, but before that the mathematical formulations of the failure and survival parameters defined above are presented as follows:

$$P_{LARBR}(ARBR \geq ARBR_c) = \frac{1}{\sqrt{2\pi}\alpha_{LARBR}} \int_{ARBRc}^{\infty} e^{-\frac{(ARBR-\mu_{LARBR})^2}{2\alpha_{LARBR}{}^2}} dARBR \tag{18}$$

$$P_{LARBR}(ARBR < ARBR_c) = \frac{1}{\sqrt{2\pi}\alpha_{LARBR}} \int_{-\infty}^{ARBRc} e^{-\frac{(ARBR-\mu_{LARBR})^2}{2\alpha_{LARBR}{}^2}} dARBR \tag{19}$$

$$P_{NLARBR}(ARBR < ARBR_c) = \frac{1}{\sqrt{2\pi}\alpha_{NLARBR}} \int_{-\infty}^{ARBRc} e^{-\frac{(ARBR-\mu_{NLARBR})^2}{2\alpha_{NLARBR}{}^2}} dARBR \tag{20}$$

$$F_{hotspots} = L \ P_{LARBR}(ARBR \geq ARBR_c) \tag{21}$$

$$SF_{hotspots} = L \ \ P_{LARBR}(ARBR < ARBR_c) \tag{22}$$

$$SS_{hotspots} = NL \ \ P_{NLARBR}(ARBR < ARBR_c) \tag{23}$$

Accordingly, the probability of casing failure **P_F ($ARBR_c$)** is defined as follows:

$$P_F(ARBR_c) = \frac{F_{hotspots}}{\left(F_{hotspots} + SF_{hotspots} + SS_{hotspots}\right)}$$

$$= \frac{L \ \ P_{LARBR}(ARBR \geq ARBR_c)}{\left(L \ \ P_{LARBR}(ARBR \geq ARBR_c) + L \ \ P_{LARBR}(ARBR < ARBR_c) + NL \ \ P_{NLARBR}(ARBR < ARBR_c)\right)} \tag{24}$$

The below figure shows the probability of casing failure plot as a function of average remaining barriers ratio cutoff.

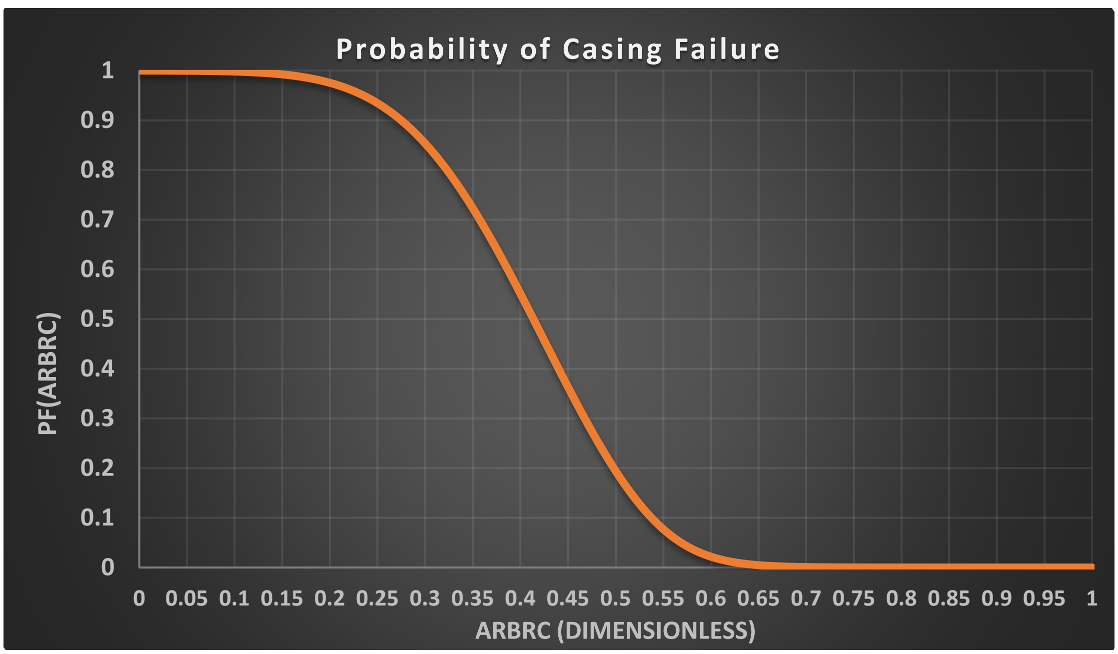

Figure 19: Probability of Casing Failure plot.

Equation (24) is an explicit mathematical expression to quantify the probability of casing failure above certain $ARBR_c$ that is cutoff based on which the decision to refer the corroded casing well to preventive maintenance workover is made. The graph in **Figure-19** shows a sharply increasing likelihood of failure below 0.65 from 0% all the way to 100% at 0.15. This equation will be one of the fundamental relationships used to obtain an optimum value of $ARBR_c$ that takes into account both risk of failure and cost of preventive maintenance workovers.

6.2 Field Casing Corrosion Distribution

In this section, we introduce the concept of field casing corrosion distribution, **P_W (ARBR)**, and model the probability of preventive maintenance and casing repair workovers, **P_{PM} ($ARBR_c$) and P_R ($ARBR_c$)** respectively.

Field casing corrosion distribution is defined as the probability density function of the lowest ARBR value in each well within a field. Another equivalent definition is that field casing corrosion distribution is the extreme value distribution of the non-leaking ARBR data. In other words, we define the lowest worst-case scenario value of ARBR in every well and collect a sample of all these values to generate the field casing corrosion distribution. Each data point in this distribution represents a well in the field or multiple fields under study. Knowing the distribution of field corrosion by well will enable the prediction of preventive maintenance and casing repair workover requirements as functions of ARBRc. So for example, if we know that the average remaining barriers ratio cutoff is 0.5 and 20% of the wells have ARBR values less than ARBRc, then we can predict that 20% of the total population of wells in a given field will be referred to preventive maintenance workover.

To generate the field casing corrosion distribution, we will start by presenting the normality test results of the extreme non-leaking data sample as follows in the below figure.

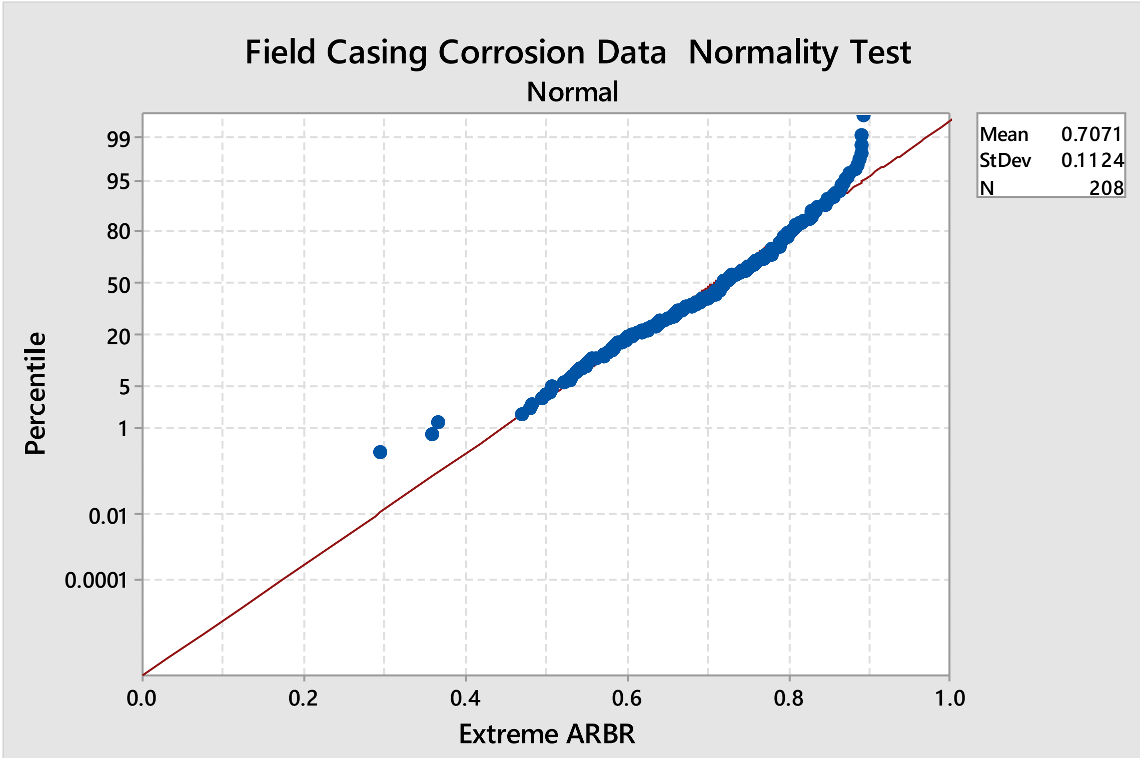

Figure 20: Field Corrosion Growth Data Normality Test.

It can be clearly seen that this plot characterizes the field corrosion growth ARBR data set as normally distributed. It is also noticed that the ARBR data deviate from normality below 0.4 and above 0.9. In statistical terms, these data may be classified as outliers but not necessarily erroneous.

After identifying the distribution, the probability density function can be written in a mathematical form to generate the Normal Probability Distribution curve. The steps followed to generate the field corrosion growth ARBR PDF curve is as follows:

1. The **non-leaking extreme hotspots** ARBR values mean and standard deviation are calculated using the below equations:

$$\mu_{NLEARBR} = \frac{\sum_{i=1}^{n}(NLEARBR)i}{n} \tag{25}$$

$$\alpha_{NLEARBR} = \sqrt{\frac{\sum_{i=1}^{n}(NLEARBRi - \mu_{NLEARBR})^2}{n-1}} \tag{26}$$

Where,

$\boldsymbol{\alpha_{NLEARBR}}$**:** Non-Leaking Extreme ARBR standard deviation.

$\boldsymbol{\mu_{NLEARBR}}$**:** Non-Leaking Extreme ARBR mean.

2. The PDF of field corrosion growth ARBR is calculated as follows:

$$P_W(ARBR) = \frac{1}{\sqrt{2\pi}\alpha_{NLEARBR}} e^{-\frac{(ARBR-\mu_{NLEARBR})^2}{2\alpha_{NLEARBR}{}^2}} \tag{27}$$

Equations (27) is plotted versus ARBR in **Figure-21** below.

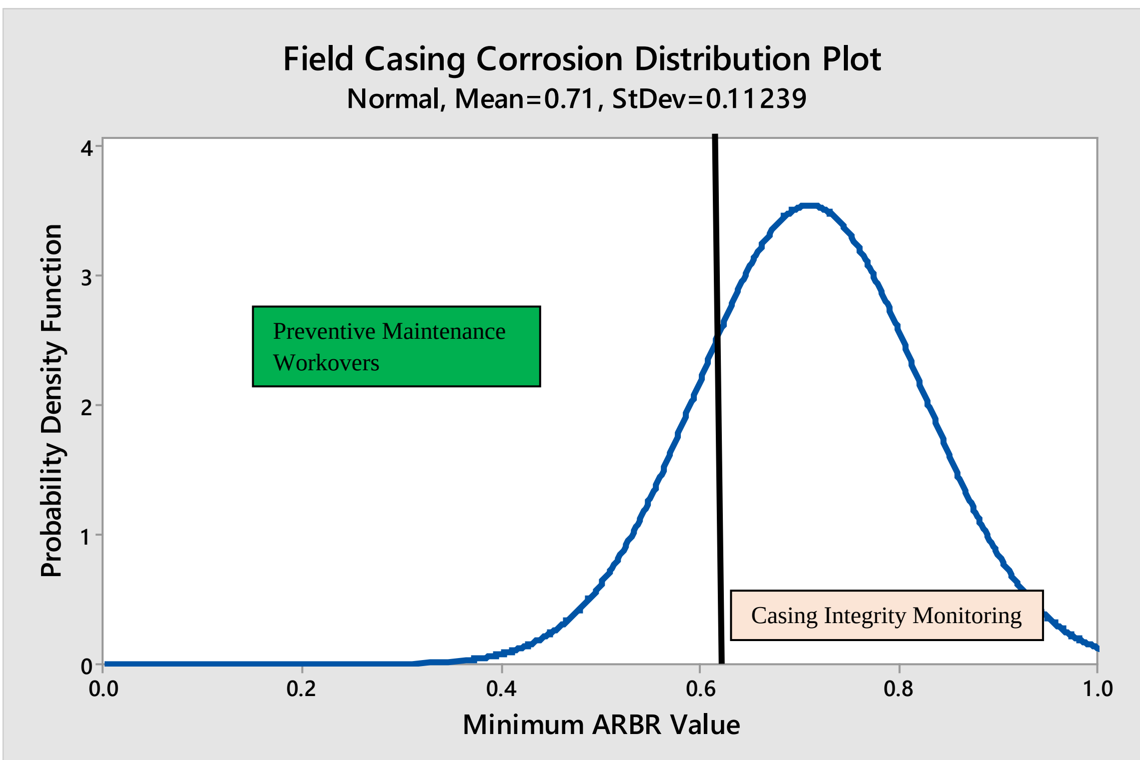

Figure 21: Field Corrosion Growth Distribution.

Figure-21 describes the field corrosion growth distribution. Generally, mature fields distributions are shifted more to the left than newer ones with better well integrity programs.

The preventive maintenance workover probability can be then written in terms of $ARBR_c$ as follows:

$$P_{PM}(ARBR_c) = P_W(ARBR < ARBR_c) =$$

$$\frac{1}{\sqrt{2\pi}\alpha_{NLEARBR}} \int_{-\infty}^{ARBRc} e^{-\frac{(ARBR-\mu_{NLEARBR})^2}{2\alpha_{NLEARBR}^2}} dARBR \qquad (28)$$

Similarly, the casing repair workover probability can be expressed in terms of $ARBR_c$ as follows:

$$P_R(ARBR_c) = P_W(ARBR \geq ARBR_c)\, P_F(ARBR_c)$$

$$= \frac{1}{\sqrt{2\pi}\alpha_{NLEARBR}} \int_{ARBRc}^{\infty} e^{-\frac{(ARBR-\mu_{NLEARBR})^2}{2\alpha_{NLEARBR}^2}} dARBR \;\; P_F(ARBR_c) \qquad (29)$$

Where P_F ($ARBR_c$) is expressed in equation (24).

Equations (28) and (29) are plotted versus $ARBR_c$ in **Figure-22** below.

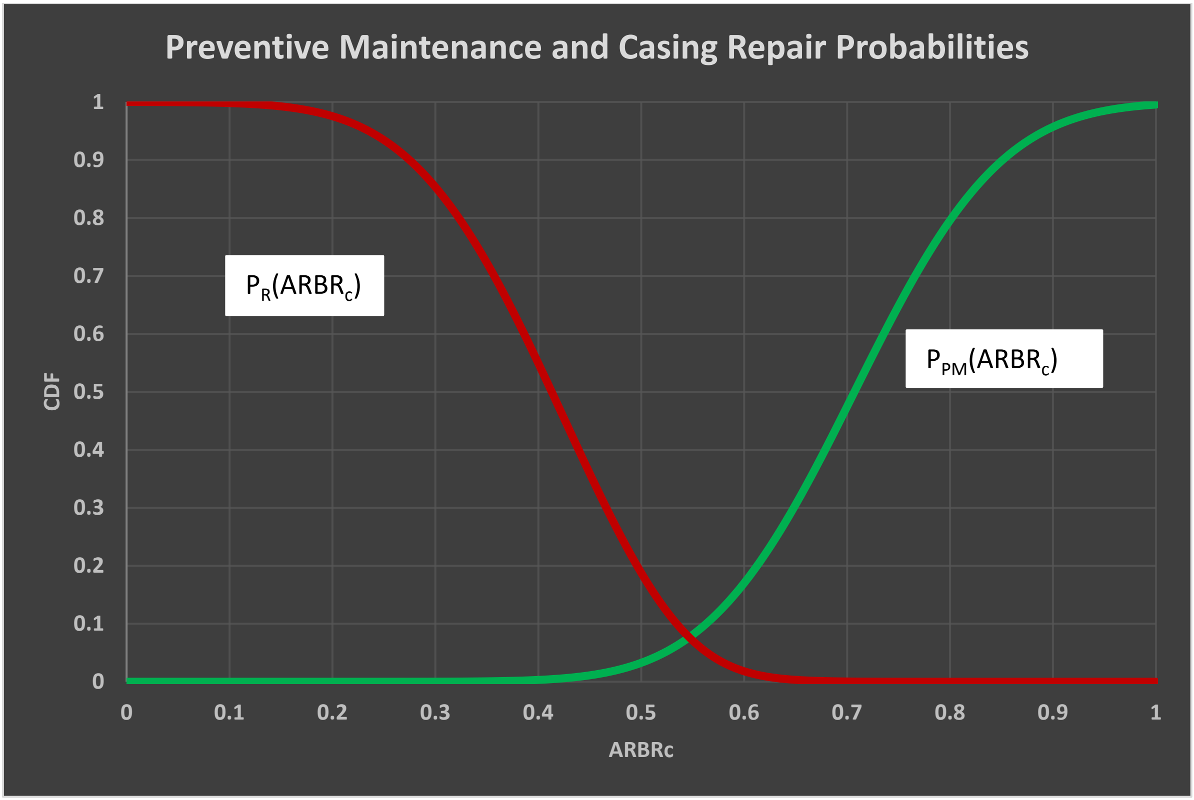

Figure 22: Preventive Maintenance and Casing Repair Probabilities.

It can be clearly seen that the higher $ARBR_c$ value we select the more preventive maintenance workovers and the less casing repair workovers there are.

Overall, the workover requirements were modeled by equations (28) and (29) based on the selected ARBRc value. The prediction of these requirements is an essential input to guide the analyst of EMIT log throughout the decision making process as to whether a well is due for workover or not.

6.3 Optimum Average Remaining Barriers Ratio ($ARBR_c^*$)

In this section, an optimum $ARBR_c$ value will be defined. The field economics element will be factored in to derive a mathematical expression that relates the expected Casing Integrity Management Cost (CIMC) with $ARBR_c$ value. Subsequently, an optimum average remaining barriers ratio ($ARBR_c^*$) is defined as the one corresponding to the minimum CIMC. The below equation describes the CIMC as a function of casing repair cost, casing repair probability, preventive maintenance cost, and preventive maintenance probability.

$$\text{Expected Casing Integrity Management Cost} = \text{Expected Casing Repair Workover Cost} + \text{Expected Preventive Maintenance Cost} \tag{30}$$

Therefore,

$$CIMC(ARBR_c) = C_R\, P_R(ARBR_c) + C_{PM}P_{PM}(ARBR_c)$$

$$= C_R\, P_W(ARBR \geq ARBR_c)P_F(ARBR_c) + C_{PM}P_W(ARBR < ARBR_c) \tag{31}$$

Equation (31) is plotted versus $ARBR_c$ in **Figure-23** below. C_R and C_{PM} values were assumed to be 4 and 2 million dollars respectively for illustration purposes; refer to Appendix D for details.

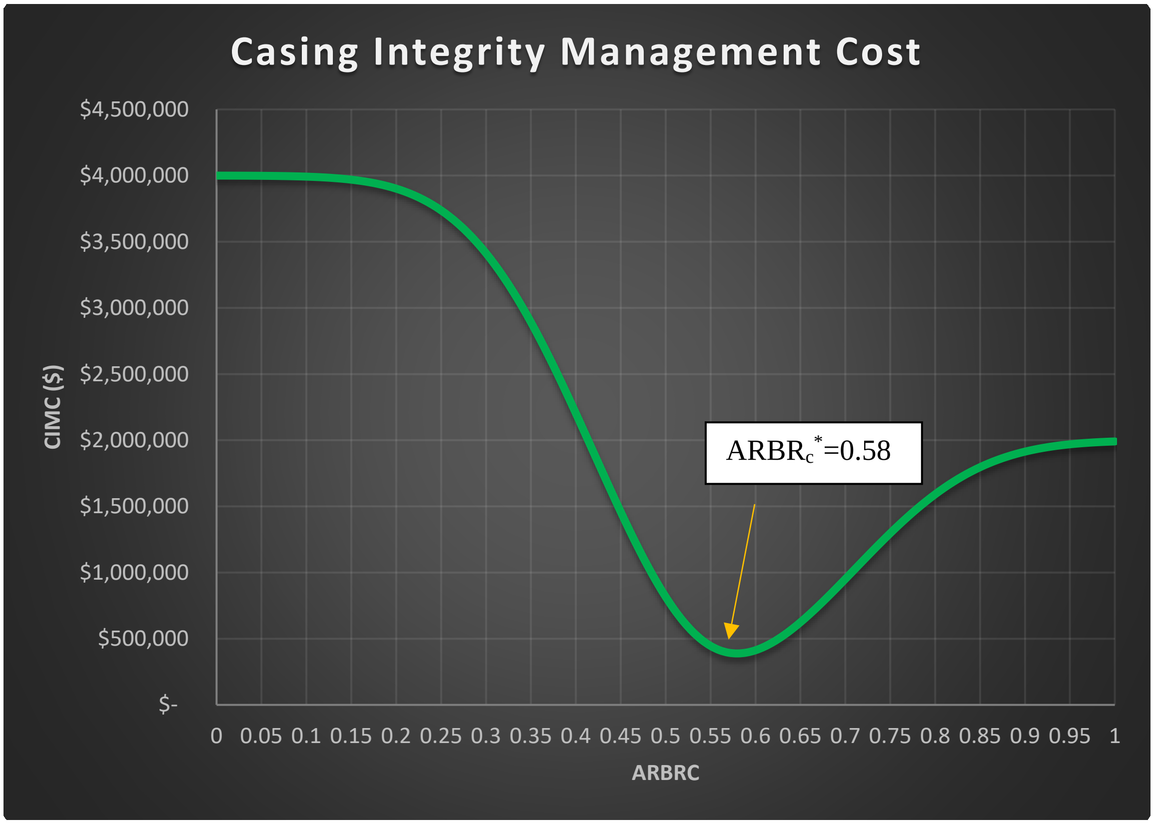

Figure 23: Casing Integrity Management Cost Curve.

In summary, $ARBR_c^*$ is dependent on the following factors:

1- Leaking ARBR distribution.
2- Non-Leaking ARBR distribution.
3- Field corrosion growth distribution.
4- Repair and preventive maintenance costs.

Equation (31) is very dynamic and changes constantly with every new EMIT log entered in the data base, casing failure incident, and/or change in workover costs.

6.4 Zero-Tolerance Average Remaining Barriers Ratio ($ARBR_0$)

In this section, we introduce the zero-tolerance decision making approach. In simple terms, the average remaining barriers ratio cutoff that corresponds to zero failure probability is defined as $ARBR_0$. This approach doesn't consider the economic implications of being too conservative in the decision making. To express this in a mathematical form, equation (31) is re-written as follows:

$$CIMC(ARBR_0) = C_R\,P_W(ARBR \geq ARBR_0)P_F(ARBR_0) + C_{PM}P_W(ARBR < ARBR_0) \qquad (32)$$

By definition, $P_F(ARBR_0) = 0$; hence, the equation becomes:

$$CIMC(ARBR_0) = C_{PM}P_W(ARBR < ARBR_0) \qquad (33)$$

Applying the Zero-Tolerance on the same example in Appendix D results in a great increase of 60.60% in the Casing Integrity Management Cost compared to the optimum scenario i.e. $CIMC(ARBR_c^*)$. **Figure-24** below illustrates this fact.

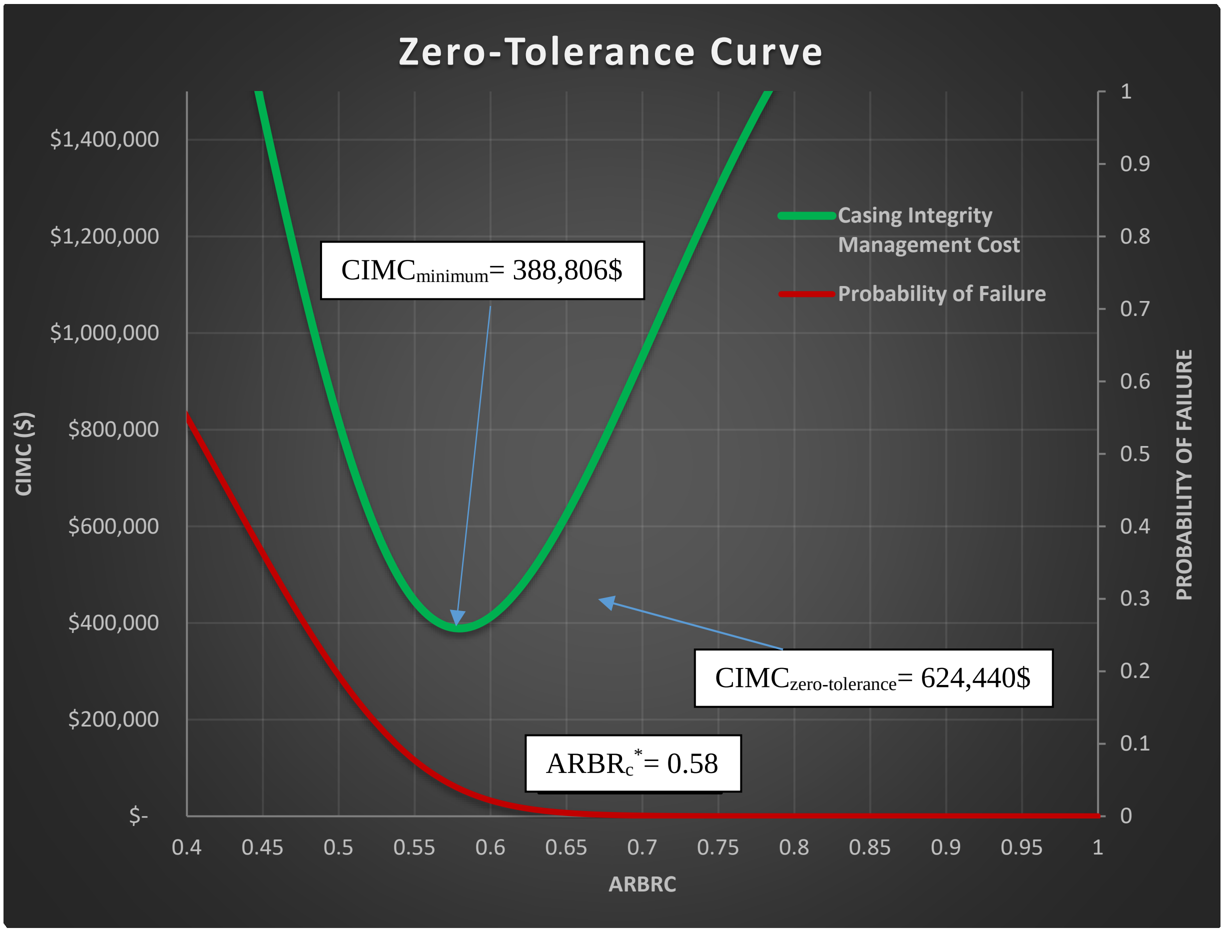

Figure 24: Zero-Tolerance Curve.

CHAPTER 7

CORROSION SURVEILLANCE DESIGN

In this chapter, we will discuss the challenges of EMIT corrosion logging frequency design and derive a statistical model to predict the casing life.

There are two sources of uncertainty in predicting the casing life; they are as follows:

- Uncertainty in retirement remaining thickness prediction. This was addressed in chapter six where the retirement thickness will be the one corresponding to $ARBR_c^*$ or $ARBR_0$ if a zero tolerance approach is applied.
- Variation of corrosion rate over time.

7.1 Casing Corrosion Monitoring Concept

The corrosion growth rate could increase, decrease, or stay constant over time depending on the nature of corrosion. Understanding the corrosion trend requires time-lapse data to verify whether the curve in **Figure 25** will concave up or down. Extrapolating the metal loss over time using a linear function to predict the expected life should be done with caution and a risk based safety factor should be applied to the expected life values particularly when the only information we have about the corrosion growth is from the base log.

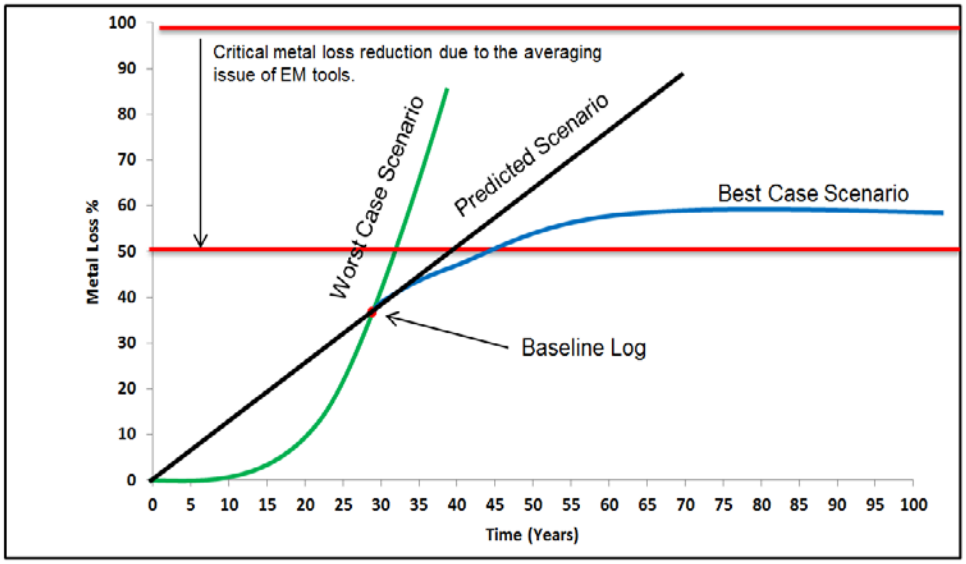

Figure 25: Uncertainty in Corrosion Growth Prediction.

7.2 Corrosion Logging Frequency Modeling

In this section, we will present statistical models to predict casing life and design corrosion logging frequency. In case adequate **time-lapse logging** is performed in a given well to profile the casing corrosion rate over time, the casing expected life can be determined after correlating EMIT average remaining thickness measurements with time. Adequate time-lapse logging means that a clear corrosion growth trend can be discerned from EMIT data over time **(see Figure 25)**.

The addressed challenge in this section of the research work is the prediction of casing expected life from **base EMIT logs**. Generally, corrosion rate variation is caused by three fundamental factors as follows:

1- Corrosion growth hotspot location. Corrosion rate varies from one well to another within the same depth interval due to differences in completion cement quality and aquifer corrosivity.
2- Corrosion growth depth interval. Similarly, completion cement quality, aquifer type, and presence of loss circulation zones changes the corrosion rate profile with depth.
3- Well age. This factor considers the variation of corrosion rate over time which is the most challenging variation to quantify in the absence of time-lapse casing corrosion logs.

Quantifying the corrosion rate variation over time is not possible without time-lapse corrosion logs. Therefore, a method is proposed to estimate that variation by studying the corrosion rate distribution in the fields understudy for given depth intervals. The proposed method is as follows:

1- Divide the corrosion rate data in a given field into subsets by depth interval. This is to minimize the corrosion rate variation due to depth. The narrower the depth interval is the less uncertainty there is in the corrosion rate variation estimate.
2- Identify the corrosion rate distribution for each depth interval.
3- Calculate the maximum likely corrosion rate value. This value is the one corresponding to a Z_{score} value of 3 after excluding statistical outliers.
4- Modify the expected life equation, eq. (4), by including this maximum likely corrosion rate.

In this research, the above steps will be applied on the data under study to derive a mathematical expression of EMIT corrosion logging frequency. Due to the limitation with regards to the data availability across all depth intervals, the method will be applied over the first 900 feet only to demonstrate the corrosion rate variation concept. The reasons behind selecting this interval are as follows:

- All the corrosive aquifers in the fields under study are above 900 feet.
- Most of the loss circulation zones and cement quality issues are within this interval.

So first, a corrosion rate data set is collected consisting of corrosion growth hotspots within the first 900 feet. A normally test is performed to identify whether this data set is normal or not. The results are presented in the below figure.

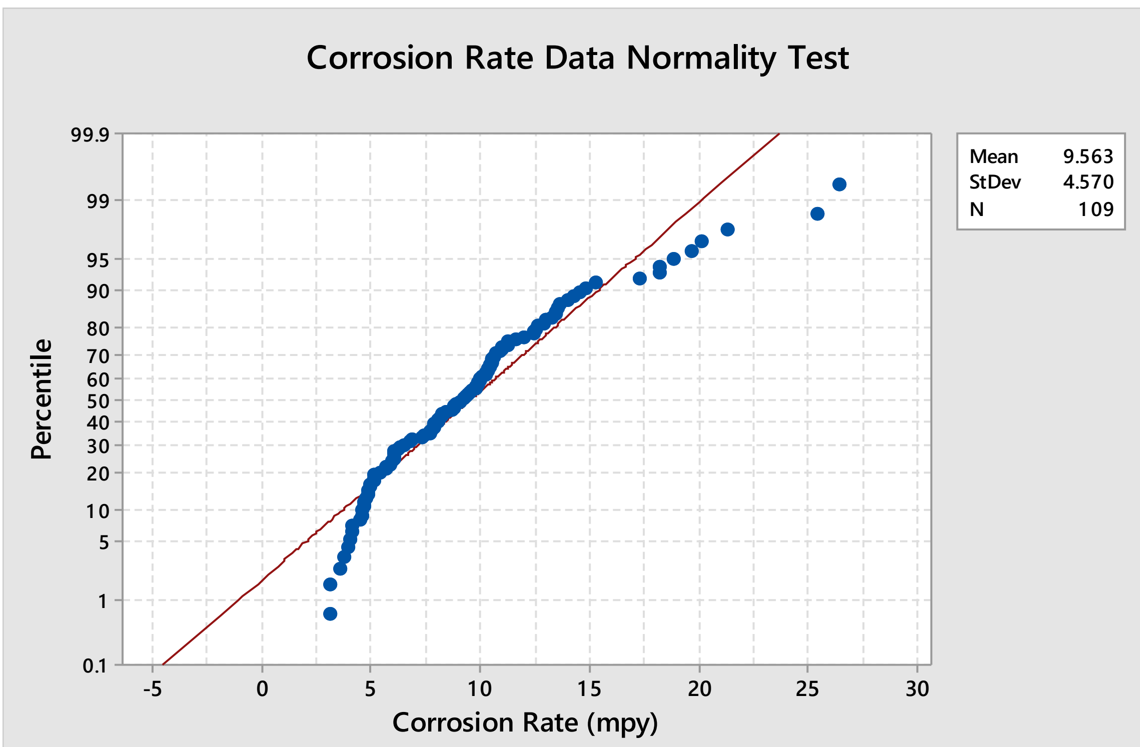

Figure 26: Corrosion Rate Normality Test.

It can be clearly seen that this plot characterizes the first 900 feet corrosion rate data set as normally distributed. It is also noticed that the data deviate from normality below 5 and above 15 mpy. In statistical terms, these data may be classified as outliers but not necessarily erroneous. After identifying the distribution, the cumulative probability distribution function is plotted in the below figure.

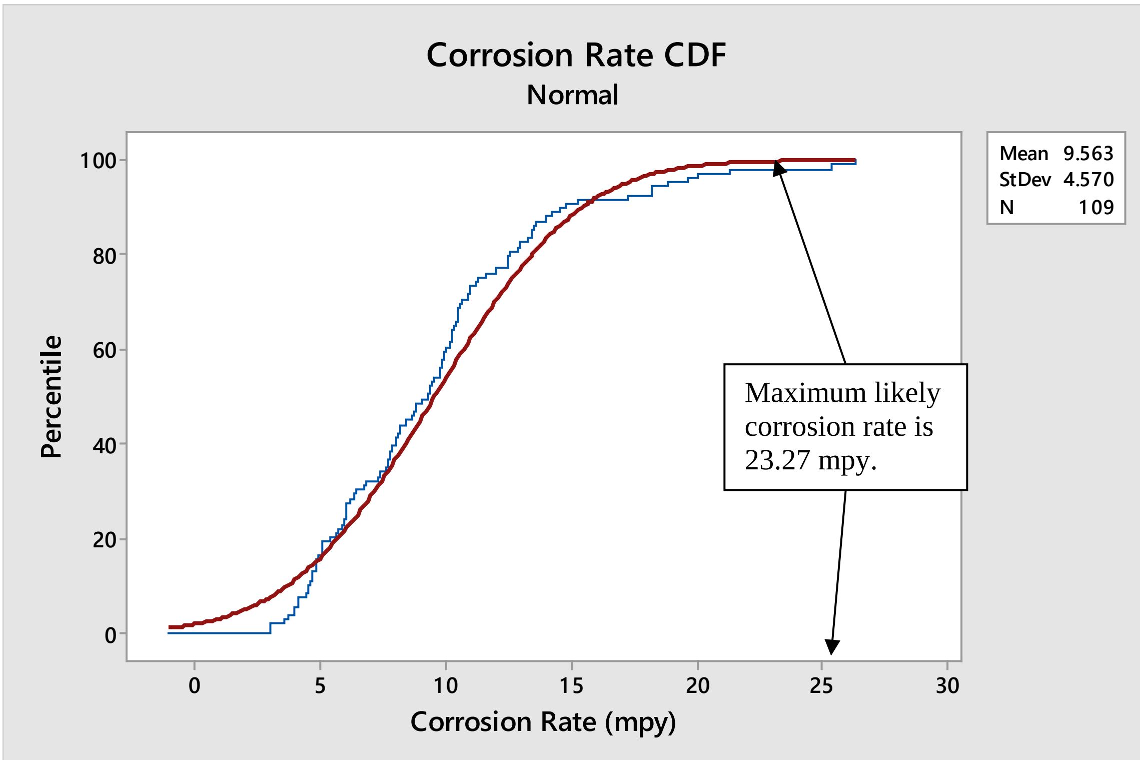

Figure 27: Corrosion Rate CDF.

Figure-27 shows a maximum likely corrosion rate of 23.27 mills per year (mpy) which is the worst-case credible corrosion rate over the studied depth interval. A mill is conventional defined as one over one thousand of an inch. This value is then used to design the corrosion logging frequency as follows:

$$CR_{z=3} = 3\,\alpha_{CR} + \mu_{CR} \tag{34}$$

$$Logging\ Frequency = \frac{[Current\ remaining\ thickness(in) - Retirment\ thickness\ (in)] \times 1000}{CR_{z=3}(mpy)} \tag{35}$$

Where,

$\boldsymbol{\alpha_{CR}}$**:** Corrosion rate standard deviation (mpy).

$\boldsymbol{\mu_{CR}}$**:** Corrosion rate mean (mpy).

Equation (35) represents a safe and conservative approach to calculate the corrosion logging frequency by considering the corrosion rate variation over time. However, it should be noted that the maximum likely corrosion rate value, determined from **Figure-27**, will continue to change with more data flow. Therefore, the corrosion logging frequency will be continuously updated depending on the corrosion rate distribution.

CHAPTER 8

RESEARCH SUMMARY, CONCLUSIONS AND AREAS FOR FURTHER INVESTIGATION

In this chapter, we will summarize the research conclusions and suggest some areas for further investigation or improvement beyond what have been achieved in this work.

8.1 Summary and Conclusions

1- Electromagnetic Induction corrosion logging technology (EMIT) uncertainty was quantified by studying the average metal loss measurements across leaking and non-leaking metal loss hotspots.

2- A new parameter, Average Remaining Barriers Ratio (ARBR), was introduced to normalize the effects of multiple casings' combinations, grades and thicknesses.

3- The assumption that average metal loss, ARBR and corrosion rate data are normally distributed is fairly applicable.

4- A probability of failure model was derived as a function of an ARBR cutoff value below which wells are referred to preventive maintained workover.

5- The probabilities of casing repair and preventive maintenance workovers were modeled as functions of the ARBR cutoff.

6- An optimum ARBR cutoff was defined whereby the overall casing integrity cost, including the preventive maintenance and casing repair costs, is minimized.

7- A zero-tolerance ARBR cutoff was defined whereby the chances of casing failure are eliminated.

8- Casing repair and preventive maintenance workover costs play a crucial role in the decision making process.

9- Zero-Tolerance approach cost can be significantly higher than the optimum ARBR approach.

10- Casing Integrity Management Cost equation is very dynamic and changes constantly with every new EMIT log entered in the data base, casing failure incident, and/or change in workover costs.

11- Generally, corrosion rate variation is caused by three fundamental factors; these are corrosion growth hotspot location, corrosion growth depth interval and well age.

12- A statistical model was formulated to predict the casing life and design the corrosion logging frequency based on base EMIT log data.

13- The methods suggested in this research work are widely applicable to analyze EMIT data irrespective of the field, well, or completion type.

14- Applying the research outcomes in the industry will enhance the well integrity surveillance program as a whole, including the use of reactive surveillance tools such as temperature surveys, annuli surveys and near surface casing inspections.

8.2 Areas for Further Investigation

The following focus areas are opportunities for further improvement in the multiple casing integrity surveillance research field:

1- Electromagnetic corrosion logging candidate selection. Data sampling method of both base and time-lapse logs can greatly affect the overall casing corrosion surveillance program. Hence, investigating the possibility of developing a risk-based sampling methodology is of importance.

2- Studying EMIT time-lapse corrosion logs to determine a correlation of corrosion growth over time and minimizing the uncertainty in forecasting the life of a casing.

3- Modifying the Casing Integrity Management Cost equation to account for the variation in workover economics.

4- Quantifying the uncertainty of and improving EMDS technology interpretation.

5- Developing a directional multiple casing corrosion profiling tool to eliminate the uncertainty associated with current technology.

APPENDIX A: EMIT DATA

Field	Well Number	Leaking Case (Yes/No)	Average ML%	Age	Average Remaining Barriers Ratio	Corrosion Rate
SD	**107**	NO	58%	43	0.470	14.824
AD	**32**	NO	41%	63	0.614	10.510
AD	**179**	NO	40%	42	0.658	10.467
AD	**179**	NO	38%	42	0.676	9.943
SD	**197**	NO	56%	34	0.505	25.365
SD	**55**	YES	60%	45	0.444	10.427
SD	**77**	YES	59%	45	0.455	10.253
AD	**98**	YES	45%	47	0.591	7.487
SD	**105**	YES	75%	42	0.264	11.946
HR	**134**	YES	40%	18	0.617	16.822
SD	**9**	NO	50%	60	0.529	9.892
AD	**155**	NO	49%	40	0.557	13.990
SD	**53**	YES	82%	46	0.095	19.591
AD	**199**	YES	44%	39	0.600	8.823
AB	**42**	YES	59%	64	0.439	10.943
SD	**63**	YES	62%	45	0.429	15.142
AD	**119**	NO	50%	41	0.554	13.402
UT	**176**	YES	69%	40	0.356	18.958
SD	**99**	YES	53%	43	0.522	13.546
SD	**105**	YES	59%	42	0.460	15.438
SD	**152**	NO	68%	41	0.366	18.227
AD	**142**	NO	52%	42	0.533	13.607
SD	**76**	NO	51%	45	0.543	12.455
SD	**82**	NO	49%	45	0.543	12.457
SD	**6**	YES	50%	61	0.529	9.730
SD	**63**	NO	51%	45	0.567	15.289
UT	**601**	NO	23%	21	0.792	17.272
SD	**457**	NO	26%	12	0.758	26.368
SD	**209**	NO	30%	33	0.708	18.227
SD	**157**	NO	40%	40	0.658	10.990
SD	**128**	NO	39%	42	0.668	10.205
AB	**845**	NO	36%	42	0.673	13.517
UT	**397**	NO	36%	38	0.682	14.533
SD	**55**	NO	43%	45	0.626	10.502

SD	**139**	NO	38%	42	0.651	12.965
SD	**153**	NO	38%	41	0.664	14.218
AD	**185**	NO	39%	40	0.639	11.573
SD	**183**	NO	39%	36	0.639	13.249
SD	**51**	NO	40%	46	0.658	9.557
SD	**294**	NO	42%	24	0.608	21.298
SD	**77**	NO	42%	45	0.637	10.257
SD	**110**	NO	42%	42	0.637	10.990
AB	**84**	NO	42%	53	0.625	9.050
AD	**209**	NO	43%	37	0.597	18.850
SD	**91**	NO	43%	42	0.626	11.252
SD	**53**	NO	43%	46	0.626	10.273
SD	**163**	NO	44%	40	0.606	12.562
AB	**862**	NO	47%	37	0.571	20.058
SD	**166**	NO	47%	40	0.585	12.913
UT	**189**	NO	47%	40	0.577	13.419
AB	**193**	NO	25%	37	0.780	10.365
AB	**62**	NO	18%	65	0.850	3.979
SD	**81**	NO	30%	45	0.744	7.327
SD	**156**	NO	13%	40	0.889	3.572
AB	**18**	NO	23%	67	0.779	3.704
SD	**88**	NO	14%	42	0.834	5.113
SD	**149**	NO	15%	41	0.868	5.612
SD	**142**	NO	15%	40	0.872	4.121
AB	**71**	NO	16%	58	0.849	4.455
AB	**192**	NO	12%	37	0.889	3.957
SD	**143**	NO	16%	41	0.882	6.064
SD	**38**	NO	19%	46	0.838	4.539
SD	**57**	NO	19%	46	0.838	4.539
AD	**90**	NO	19%	45	0.838	4.640
SD	**131**	NO	18%	41	0.847	4.825
AD	**141**	NO	18%	42	0.847	4.710
SD	**125**	NO	19%	42	0.842	4.850
SD	**50**	NO	20%	45	0.830	4.884
SD	**16**	NO	24%	61	0.779	4.670
SD	**14**	NO	24%	58	0.779	4.912
SD	**83**	NO	22%	45	0.820	7.744
AB	**179**	NO	24%	37	0.768	8.173
SD	**80**	NO	25%	55	0.771	5.373

SD	**52**	NO	24%	47	0.788	7.833
AD	**7**	NO	28%	65	0.661	6.190
SD	**104**	NO	23%	42	0.804	6.018
AB	**604**	NO	10%	27	0.908	6.030
AD	**151**	NO	23%	41	0.814	7.809
AD	**151**	NO	23%	41	0.709	7.809
SD	**173**	NO	22%	36	0.813	6.716
SD	**56**	NO	25%	46	0.787	5.973
UT	**415**	NO	23%	37	0.792	9.803
UT	**542**	NO	23%	35	0.794	10.403
AB	**915**	NO	16%	18	0.853	10.551
SD	**930**	NO	22%	31	0.780	3.052
SD	**930**	NO	22%	31	0.780	3.052
SD	**305**	NO	19%	21	0.829	11.237
SD	**156**	NO	27%	40	0.770	7.418
AD	**47**	NO	33%	62	0.696	6.318
SD	**201**	NO	26%	33	0.778	8.659
SD	**111**	NO	31%	44	0.730	6.475
SD	**160**	NO	30%	39	0.734	8.785
SD	**910**	NO	20%	34	0.801	5.088
SD	**108**	NO	32%	43	0.727	8.179
AD	**199**	NO	31%	39	0.736	8.736
SD	**54**	NO	33%	45	0.719	8.059
SD	**140**	NO	33%	45	0.719	8.059
SD	**49**	NO	34%	46	0.710	8.123
AD	**98**	NO	32%	35	0.727	10.048
SD	**93**	NO	36%	42	0.693	9.420
SD	**175**	NO	36%	37	0.693	10.693
SF	**29**	NO	27%	56	0.737	6.041
SF	**29**	NO	24%	56	0.779	5.087
SF	**92**	NO	18%	48	0.847	4.121
SF	**246**	NO	27%	33	0.758	9.472
SF	**246**	NO	27%	33	0.761	9.347
SF	**246**	NO	27%	33	0.763	9.264
SF	**278**	NO	26%	33	0.774	8.822
SF	**280**	NO	35%	33	0.693	12.001
SF	**280**	NO	30%	33	0.737	10.292
SF	**280**	NO	29%	33	0.747	9.887
SF	**280**	NO	28%	33	0.750	9.776

SF	**368**	NO	11%	30	0.885	7.674
SF	**379**	NO	18%	31	0.821	7.641
SF	**426**	NO	15%	29	0.872	5.684
SF	**476**	NO	13%	28	0.874	5.850
SF	**483**	NO	24%	28	0.767	10.860
SF	**483**	NO	22%	28	0.786	9.955
SF	**488**	NO	18%	28	0.819	8.421
SF	**490**	NO	42%	28	0.587	19.650
SF	**502**	NO	12%	23	0.880	6.835
SF	**704**	NO	21%	22	0.789	12.505

Table 4: EMIT Data

APPENDIX B: FIELD CORROSION GROWTH DATA

(EQUATION# 27)

Number of Wells (W)		
208		
Field	**Well Number**	**ARBR**
AB	18	0.78
AB	62	0.75
AB	63	0.72
AB	71	0.71
AB	72	0.48
AB	73	0.70
AB	84	0.30
AB	106	0.72
AB	110	0.64
AB	145	0.71
AB	179	0.72
AB	192	0.81
AB	193	0.78
AB	198	0.81
AB	232	0.56
AB	271	0.54
AB	314	0.70
AB	604	0.61
AB	605	0.60
AB	845	0.67
AB	862	0.57
AB	915	0.76
AB	924	0.86
AD	1	0.74
AD	5	0.77
AD	7	0.66
AD	31	0.65
AD	32	0.61
AD	46	0.36
AD	47	0.66
AD	78	0.53
AD	85	0.80

AD	90	0.70
AD	98	0.73
AD	99	0.64
AD	119	0.55
AD	123	0.81
AD	135	0.78
AD	141	0.85
AD	142	0.53
AD	151	0.71
AD	155	0.56
AD	157	0.83
AD	167	0.74
AD	185	0.64
AD	199	0.74
AD	209	0.60
AD	211	0.71
AD	222	0.67
AD	235	0.77
AD	242	0.75
AD	257	0.66
SD	6	0.89
SD	8	0.75
SD	9	0.53
SD	14	0.72
SD	16	0.78
SD	22	0.76
SD	30	0.71
SD	38	0.79
SD	40	0.66
SD	41	0.86
SD	49	0.71
SD	50	0.83
SD	51	0.66
SD	52	0.72
SD	53	0.63
SD	54	0.72
SD	55	0.63
SD	56	0.79
SD	57	0.71
SD	64	0.73
SD	67	0.86

SD	76	0.54
SD	77	0.64
SD	80	0.71
SD	81	0.62
SD	82	0.50
SD	83	0.82
SD	88	0.83
SD	91	0.63
SD	93	0.69
SD	104	0.80
SD	107	0.47
SD	108	0.73
SD	111	0.73
SD	114	0.80
SD	125	0.67
SD	126	0.77
SD	127	0.73
SD	128	0.67
SD	131	0.85
SD	136	0.78
SD	137	0.84
SD	138	0.87
SD	139	0.65
SD	140	0.72
SD	143	0.80
SD	149	0.87
SD	150	0.75
SD	152	0.37
SD	153	0.66
SD	156	0.77
SD	160	0.73
SD	163	0.61
SD	166	0.58
SD	173	0.70
SD	175	0.69
SD	177	0.81
SD	183	0.64
SD	186	0.89
SD	188	0.55
SD	190	0.71
SD	195	0.85

SD	197	0.51
SD	201	0.78
SD	203	0.74
SD	206	0.55
SD	218	0.76
SD	219	0.83
SD	292	0.79
SD	294	0.61
SD	303	0.89
SD	305	0.83
SD	457	0.76
SD	731	0.89
SD	910	0.63
SD	930	0.78
SF	29	0.69
SF	60	0.72
SF	86	0.75
SF	92	0.85
SF	112	0.54
SF	121	0.69
SF	148	0.62
SF	154	0.81
SF	172	0.48
SF	174	0.52
SF	240	0.59
SF	241	0.76
SF	243	0.80
SF	244	0.76
SF	246	0.76
SF	261	0.71
SF	270	0.78
SF	272	0.64
SF	277	0.68
SF	278	0.55
SF	280	0.69
SF	308	0.72
SF	309	0.68
SF	310	0.75
SF	317	0.66
SF	343	0.66
SF	344	0.83

SF	349	0.72
SF	350	0.54
SF	351	0.72
SF	357	0.65
SF	362	0.89
SF	365	0.51
SF	366	0.73
SF	368	0.88
SF	370	0.58
SF	371	0.58
SF	374	0.49
SF	379	0.60
SF	426	0.87
SF	427	0.87
SF	435	0.60
SF	436	0.79
SF	443	0.67
SF	446	0.78
SF	448	0.77
SF	449	0.79
SF	450	0.81
SF	460	0.57
SF	470	0.80
SF	471	0.86
SF	474	0.82
SF	475	0.83
SF	476	0.87
SF	479	0.72
SF	483	0.75
SF	485	0.64
SF	488	0.58
SF	490	0.58
SF	491	0.66
SF	495	0.59
SF	498	0.76
SF	502	0.51
SF	576	0.81
SF	593	0.88
SF	594	0.59
SF	646	0.82
SF	704	0.68

UT	189	0.58
UT	301	0.89
UT	397	0.68
UT	415	0.79
UT	431	0.59
UT	466	0.85
UT	542	0.79
UT	568	0.83
UT	601	0.79
UT	614	0.79
UT	1179	0.79
UT	1208	0.79

Table 5: Field Corrosion Growth Data

APPENDIX C: PROBABILITY OF CASING FAILURE DATA (EQUATION# 24)

L	NL			
37	498			
ARBRc	**PLARBR(ARBR>=ARBRc)**	**PLARBR(ARBR<ARBRc)**	**PNLARBR(ARBR<ARBRc)**	**PF(ARBRc)**
0	0.999925706	7.42937E-05	6.3372E-13	0.999925706
0.01	0.999893051	0.000106949	1.25405E-12	0.999893051
0.02	0.999847257	0.000152743	2.45971E-12	0.999847257
0.03	0.999783571	0.000216429	4.78202E-12	0.999783571
0.04	0.99969574	0.00030426	9.21503E-12	0.99969574
0.05	0.999575615	0.000424385	1.76012E-11	0.999575615
0.06	0.99941269	0.00058731	3.33235E-11	0.99941269
0.07	0.999193553	0.000806447	6.25349E-11	0.999193552
0.08	0.99890126	0.00109874	1.16322E-10	0.998901258
0.09	0.99851463	0.00148537	2.14471E-10	0.998514627
0.1	0.99800747	0.00199253	3.91964E-10	0.998007464
0.11	0.997347734	0.002652266	7.10064E-10	0.997347725
0.12	0.996496659	0.003503341	1.27504E-09	0.996496642
0.13	0.99540788	0.00459212	2.2695E-09	0.99540785
0.14	0.994026588	0.005973412	4.00421E-09	0.994026535
0.15	0.992288767	0.007711233	7.00304E-09	0.992288674
0.16	0.990120572	0.009879428	1.21407E-08	0.990120411
0.17	0.987437913	0.012562087	2.08637E-08	0.987437636
0.18	0.984146317	0.015853683	3.55411E-08	0.984145846
0.19	0.980141143	0.019858857	6.00159E-08	0.980140351

0.2	0.975308218	0.024691782	1.00462E-07	0.975306899
0.21	0.969524959	0.030475041	1.66702E-07	0.969522784
0.22	0.962662039	0.037337961	2.74212E-07	0.962658486
0.23	0.954585614	0.045414386	4.47141E-07	0.954579869
0.24	0.94516014	0.05483986	7.22796E-07	0.945150946
0.25	0.934251741	0.065748259	1.15826E-06	0.934237176
0.26	0.921732075	0.078267925	1.84002E-06	0.921709249
0.27	0.90748262	0.09251738	2.89779E-06	0.907447227
0.28	0.891399229	0.108600771	4.52422E-06	0.891344952
0.29	0.873396812	0.126603188	7.0026E-06	0.873314501
0.3	0.853413942	0.146586058	1.07453E-05	0.853290534
0.31	0.831417181	0.168582819	1.63467E-05	0.831234296
0.32	0.807404899	0.192595101	2.46544E-05	0.807137063
0.33	0.781410368	0.218589632	3.68656E-05	0.781022831
0.34	0.753503933	0.246496067	5.46535E-05	0.752950058
0.35	0.723794074	0.276205926	8.03321E-05	0.723012333
0.36	0.692427243	0.307572757	0.000117069	0.691337907
0.37	0.659586381	0.340413619	0.000169157	0.658088076
0.38	0.625488117	0.374511883	0.000242344	0.623454521
0.39	0.590378683	0.409621317	0.000344258	0.587655767
0.4	0.554528676	0.445471324	0.000484899	0.550933027
0.41	0.518226848	0.481773152	0.000677242	0.513545717
0.42	0.481773152	0.518226848	0.000937936	0.475767016
0.43	0.445471324	0.554528676	0.001288098	0.437879756
0.44	0.409621317	0.590378683	0.001754215	0.400172923

0.45	0.374511883	0.625488117	0.002369116	0.362938846
0.46	0.340413619	0.659586381	0.003173016	0.326470994
0.47	0.307572757	0.692427243	0.00421458	0.291061985
0.48	0.276205926	0.723794074	0.005551961	0.257001155
0.49	0.246496067	0.753503933	0.007253771	0.224570807
0.5	0.218589632	0.781410368	0.009399886	0.194040177
0.51	0.192595101	0.807404899	0.012082022	0.165656463
0.52	0.168582819	0.831417181	0.015403988	0.139632834
0.53	0.146586058	0.853413942	0.019481502	0.116134401
0.54	0.126603188	0.873396812	0.024441506	0.095264182
0.55	0.108600771	0.891399229	0.030420866	0.077051965
0.56	0.09251738	0.90748262	0.037564409	0.061448981
0.57	0.078267925	0.921732075	0.046022234	0.048330408
0.58	0.065748259	0.934251741	0.055946307	0.037505987
0.59	0.05483986	0.94516014	0.067486348	0.028737098
0.6	0.045414386	0.954585614	0.080785101	0.021757231
0.61	0.037337961	0.962662039	0.095973105	0.016292364
0.62	0.030475041	0.969524959	0.113163135	0.012078342
0.63	0.024691782	0.975308218	0.132444542	0.008873535
0.64	0.019858857	0.980141143	0.153877743	0.006466342
0.65	0.015853683	0.984146317	0.177489129	0.00467811
0.66	0.012562087	0.987437913	0.203266707	0.003362569
0.67	0.009879428	0.990120572	0.231156734	0.002403026
0.68	0.007711233	0.992288767	0.261061604	0.001708388
0.69	0.005973412	0.994026588	0.292839204	0.001208836

0.7	0.00459212	0.99540788	0.326303865	0.000851674
0.71	0.003503341	0.996496659	0.361228988	0.000597641
0.72	0.002652266	0.997347734	0.397351309	0.000417802
0.73	0.00199253	0.99800747	0.434376689	0.00029103
0.74	0.00148537	0.99851463	0.47198723	0.000202017
0.75	0.00109874	0.99890126	0.509849426	0.000139748
0.76	0.000806447	0.999193553	0.547623011	9.63415E-05
0.77	0.00058731	0.99941269	0.584970103	6.61878E-05
0.78	0.000424385	0.999575615	0.621564244	4.53116E-05
0.79	0.00030426	0.99969574	0.657098931	3.09076E-05
0.8	0.000216429	0.999783571	0.691295269	2.10034E-05
0.81	0.000152743	0.999847257	0.72390843	1.42173E-05
0.82	0.000106949	0.999893051	0.754732669	9.58468E-06
0.83	7.42937E-05	0.999925706	0.783604745	6.43408E-06
0.84	5.12015E-05	0.999948798	0.810405674	4.2999E-06
0.85	3.50076E-05	0.999964992	0.835060834	2.86022E-06
0.86	2.37457E-05	0.999976254	0.857538541	1.89329E-06
0.87	1.59787E-05	0.999984021	0.877847252	1.24684E-06
0.88	1.06667E-05	0.999989333	0.896031648	8.16742E-07
0.89	7.06393E-06	0.999992936	0.91216786	5.32031E-07
0.9	4.64067E-06	0.999995359	0.926358124	3.44563E-07
0.91	3.02435E-06	0.999996976	0.938725157	2.21812E-07
0.92	1.95521E-06	0.999998045	0.949406521	1.41903E-07
0.93	1.25389E-06	0.999998746	0.958549214	9.01982E-08
0.94	7.97685E-07	0.999999202	0.966304677	5.69533E-08
0.95	5.03384E-07	0.999999497	0.972824375	3.5717E-08
0.96	3.1511E-07	0.999999685	0.978256045	2.22429E-08
0.97	1.95666E-07	0.999999804	0.982740663	1.3753E-08
0.98	1.20519E-07	0.999999879	0.986410136	8.44178E-09
0.99	7.36346E-08	0.999999926	0.989385693	5.1433E-09
1	4.46259E-08	0.999999955	0.991776908	3.11008E-09

Table 6: Probability of Casing Failure Data

APPENDIX D: CASING INTEGRITY MANAGEMENT COST DATA (EQUATION# 31)

CR	CPM
$ 4,000,000	$ 2,000,000

ARBRc	PPM(ARBRc)	PF(ARBRc)	PR(ARBRc)	CIMC ($)
0	1.5779E-10	0.999925706	0.999925706	$ 3,999,703
0.01	2.78826E-10	0.999893051	0.999893051	$ 3,999,572
0.02	4.8891E-10	0.999847257	0.999847257	$ 3,999,389
0.03	8.5068E-10	0.999783571	0.99978357	$ 3,999,134
0.04	1.46875E-09	0.99969574	0.999695738	$ 3,998,783
0.05	2.51638E-09	0.999575615	0.999575612	$ 3,998,302
0.06	4.27812E-09	0.99941269	0.999412686	$ 3,997,651
0.07	7.2174E-09	0.999193552	0.999193545	$ 3,996,774
0.08	1.20826E-08	0.998901258	0.998901246	$ 3,995,605
0.09	2.00724E-08	0.998514627	0.998514607	$ 3,994,058
0.1	3.30899E-08	0.998007464	0.998007431	$ 3,992,030
0.11	5.41318E-08	0.997347725	0.997347671	$ 3,989,391
0.12	8.78766E-08	0.996496642	0.996496554	$ 3,985,986
0.13	1.41567E-07	0.99540785	0.995407709	$ 3,981,631
0.14	2.26318E-07	0.994026535	0.99402631	$ 3,976,106
0.15	3.59046E-07	0.992288674	0.992288318	$ 3,969,154
0.16	5.65272E-07	0.990120411	0.990119851	$ 3,960,481
0.17	8.83172E-07	0.987437636	0.987436764	$ 3,949,749
0.18	1.36936E-06	0.984145846	0.984144499	$ 3,936,581
0.19	2.10705E-06	0.980140351	0.980138286	$ 3,920,557
0.2	3.21754E-06	0.975306899	0.975303761	$ 3,901,221
0.21	4.87606E-06	0.969522784	0.969518056	$ 3,878,082
0.22	7.33353E-06	0.962658486	0.962651426	$ 3,850,620
0.23	1.09462E-05	0.954579869	0.95456942	$ 3,818,300
0.24	1.62151E-05	0.945150946	0.94513562	$ 3,780,575
0.25	2.38391E-05	0.934237176	0.934214905	$ 3,736,907
0.26	3.47841E-05	0.921709249	0.921677188	$ 3,686,778
0.27	5.03726E-05	0.907447227	0.907401517	$ 3,629,707
0.28	7.24E-05	0.891344952	0.891280419	$ 3,565,266
0.29	0.000103281	0.873314501	0.873224305	$ 3,493,104
0.3	0.000146231	0.853290534	0.853165756	$ 3,412,955
0.31	0.0002055	0.831234296	0.831063477	$ 3,324,665
0.32	0.000286641	0.807137063	0.806905705	$ 3,228,196

0.33	0.00039685	0.781022831	0.780712882	$	3,123,645
0.34	0.000545364	0.752950058	0.752539426	$	3,011,248
0.35	0.000743917	0.723012333	0.722474473	$	2,891,386
0.36	0.001007277	0.691337907	0.690641539	$	2,764,581
0.37	0.001353846	0.658088076	0.657197126	$	2,631,496
0.38	0.001806321	0.623454521	0.622328362	$	2,492,926
0.39	0.002392409	0.587655767	0.586249854	$	2,349,784
0.4	0.003145586	0.550933027	0.54920002	$	2,203,091
0.41	0.004105859	0.513545717	0.511437171	$	2,053,960
0.42	0.005320528	0.475767016	0.473235684	$	1,903,584
0.43	0.006844881	0.437879756	0.434882521	$	1,753,220
0.44	0.008742801	0.400172923	0.396674291	$	1,604,183
0.45	0.011087219	0.362938846	0.358914864	$	1,457,834
0.46	0.013960358	0.326470994	0.321913342	$	1,315,574
0.47	0.017453715	0.291061985	0.285981872	$	1,178,835
0.48	0.021667711	0.257001155	0.251432529	$	1,049,066
0.49	0.026710954	0.224570807	0.218572306	$	927,711
0.5	0.032699073	0.194040177	0.187695243	$	816,179
0.51	0.039753075	0.165656463	0.159071109	$	715,791
0.52	0.047997216	0.139632834	0.132930847	$	627,718
0.53	0.057556382	0.116134401	0.109450125	$	552,913
0.54	0.068553003	0.095264182	0.088733536	$	492,040
0.55	0.081103565	0.077051965	0.070802776	$	445,418
0.56	0.0953148	0.061448981	0.055591984	$	412,998
0.57	0.111279662	0.048330408	0.042952216	$	394,368
0.58	0.129073236	0.037505987	0.032664968	$	388,806
0.59	0.148748742	0.028737098	0.024462491	$	395,347
0.6	0.170333805	0.021757231	0.018051239	$	412,873
0.61	0.193827181	0.016292364	0.013134461	$	440,192
0.62	0.219196116	0.012078342	0.009430816	$	476,115
0.63	0.246374507	0.008873535	0.006687322	$	519,498
0.64	0.275262006	0.006466342	0.004686404	$	569,270
0.65	0.305724176	0.00467811	0.003247899	$	624,440
0.66	0.337593762	0.003362569	0.002227387	$	684,097
0.67	0.370673092	0.002403026	0.001512289	$	747,395
0.68	0.404737565	0.001708388	0.001016939	$	813,543
0.69	0.439540139	0.001208836	0.000677504	$	881,790
0.7	0.474816658	0.000851674	0.000447285	$	951,422
0.71	0.510291853	0.000597641	0.00029267	$	1,021,754
0.72	0.545685764	0.000417802	0.000189814	$	1,092,131
0.73	0.580720352	0.00029103	0.000122023	$	1,161,929

0.74	0.615126033	0.000202017	7.77511E-05	$	1,230,563
0.75	0.648647886	0.000139748	4.91007E-05	$	1,297,492
0.76	0.681051284	9.63415E-05	3.0728E-05	$	1,362,225
0.77	0.712126761	6.61878E-05	1.90537E-05	$	1,424,330
0.78	0.741693929	4.53116E-05	1.17043E-05	$	1,483,435
0.79	0.769604349	3.09076E-05	7.12097E-06	$	1,539,237
0.8	0.795743272	2.10034E-05	4.29009E-06	$	1,591,504
0.81	0.820030263	1.42173E-05	2.55869E-06	$	1,640,071
0.82	0.842418734	9.58468E-06	1.51037E-06	$	1,684,844
0.83	0.862894485	6.43408E-06	8.82148E-07	$	1,725,792
0.84	0.881473383	4.2999E-06	5.09652E-07	$	1,762,949
0.85	0.89819833	2.86022E-06	2.91176E-07	$	1,796,398
0.86	0.913135704	1.89329E-06	1.64459E-07	$	1,826,272
0.87	0.92637145	1.24684E-06	9.18033E-08	$	1,852,743
0.88	0.938007011	8.16742E-07	5.06323E-08	$	1,876,014
0.89	0.948155255	5.32031E-07	2.7583E-08	$	1,896,311
0.9	0.956936562	3.44563E-07	1.48381E-08	$	1,913,873
0.91	0.964475187	2.21812E-07	7.87983E-09	$	1,928,950
0.92	0.970895997	1.41903E-07	4.12994E-09	$	1,941,792
0.93	0.976321651	9.01982E-08	2.13574E-09	$	1,952,643
0.94	0.980870266	5.69533E-08	1.0895E-09	$	1,961,741
0.95	0.984653567	3.5717E-08	5.48129E-10	$	1,969,307
0.96	0.987775527	2.22429E-08	2.71908E-10	$	1,975,551
0.97	0.990331454	1.3753E-08	1.32972E-10	$	1,980,663
0.98	0.992407487	8.44178E-09	6.40943E-11	$	1,984,815
0.99	0.994080444	5.1433E-09	3.0446E-11	$	1,988,161
1	0.995417963	3.11008E-09	1.42505E-11	$	1,990,836

Table 7: Casing Integrity Cost Management Data

NOMENCLATURE

$\boldsymbol{P_F(ARBR_c)}$**:** Probability of casing failure above a certain average remaining barriers ratio cutoff.

$\boldsymbol{P_{LARBR}(LARBR)}$**:** Leaking ARBR Probability Density Function.

$\boldsymbol{P_{LML}(LML)}$**:** Leaking Metal Loss Probability Density Function.

$\boldsymbol{P_{NLARBR}(NLARBR)}$**:** Non-Leaking ARBR Probability Density Function.

$\boldsymbol{P_{NLML}(NLML)}$**:** Non-Leaking Metal Loss Probability Density Function.

$\boldsymbol{P_R(ARBR_c)}$**:** Probability of casing repair workovers.

$\boldsymbol{\alpha_{CR}}$**:** Corrosion rate standard deviation (mpy).

$\boldsymbol{\alpha_{LARBR}}$**:** Leaking ARBR standard deviation.

$\boldsymbol{\alpha_{LML}}$**:** Leaking Metal Loss standard deviation (%).

$\boldsymbol{\alpha_{NLARBR}}$**:** Non-Leaking ARBR standard deviation.

$\boldsymbol{\alpha_{NLEARBR}}$**:** Non-Leaking Extreme ARBR standard deviation.

$\boldsymbol{\alpha_{NLML}}$**:** Non-Leaking Metal Loss standard deviation (%).

$\boldsymbol{\mu_{CR}}$**:** Corrosion rate mean (mpy).

$\boldsymbol{\mu_{LARBR}}$**:** Leaking ARBR mean.

$\boldsymbol{\mu_{LML}}$**:** Leaking Metal Loss mean (%).

$\boldsymbol{\mu_{NLARBR}}$**:** Non-Leaking ARBR mean.

$\boldsymbol{\mu_{NLEARBR}}$**:** Non-Leaking Extreme ARBR mean.

$\boldsymbol{\mu_{NLML}}$**:** Non-Leaking Metal Loss mean (%).

$\emptyset$**:** Phase shift.

ARBR: Average Remaining Barriers Ratio (dimensionless).

$\mathbf{ARBR_0}$: Zero-Tolerance Average Remaining Barriers Ratio Cutoff.

$\mathbf{ARBR_c}$: is the cutoff value at and above which the probability of casing failure is computed.

$\mathbf{ARBR_c^*}$: Optimum Average Remaining Barriers Ratio Cutoff.

$ARBR_c$: Average Remaining Barriers Ratio Cutoff.

CDF: Cumulative Distribution Function.

CIMC: Casing Integrity Management Cost.

C_{PM}: Casing preventive maintenance workover cost.

C_R: Casing repair workover cost.

$CR_{z=3}$: Maximum likely corrosion rate (mpy).

D: Depth (cm).

EM: Electromagnetic.

EMDS: Electromagnetic Defectoscope Tools.

EMIT: Electromagnetic Induction Tools.

F: Frequency (cycles per second).

$F_{hotspots}$: is the number of leaking/ failed hotspots at and above $ARBR_c$.

L: is the total number of leaking hotspots.

LARBR: Leaking Average Remaining Barriers Ratio.

LML: Leaking Metal Loss.

n: number of sample data points.

NL: is the total number of non-leaking hotspots.

NLARBR: Non-Leaking Average Remaining Barriers Ratio.

NLEARBR: Non-Leaking Extreme Average Remaining Barriers Ratio.

NLML: Non-Leaking Metal Loss.

PDF: Probability Density Function.

P_{PM} ($ARBR_c$): Probability of preventive maintenance workover.

P_W (ARBR): Probability density function of the field corrosion growth distribution.

$SF_{hotspots}$: is the number of leaking/ failed hotspots below $ARBR_c$. The "SF" notion means that these hotspots survived from failure at and above $ARBR_c$ and failed below it.

$SS_{hotspots}$: is the number of non-leaking hotspots below $ARBR_c$. The "SS" notion means that these hotspots survived from failure at and above $ARBR_c$ and still surviving below it.

T_{L1}: Thickness loss from the outer string (in).

T_{L2}: Thickness loss from the second outer string (in).

$\mathbf{T_{L3}}$**:** Thickness loss from the third outer string (in).

$\mathbf{T_{N1}}$**:** Nominal thickness of the outer string (in).

$\mathbf{T_{N2}}$**:** Nominal thickness of the second outer string (in).

$\mathbf{T_{N3}}$**:** Nominal thickness of the third outer string (in).

X: Number of strings across the hotspot.

$\boldsymbol{\mu}$**:** Relative permeability.

$\boldsymbol{\rho}$**:** Resistivity (micro-ohm cm).

REFERENCES

1. (2016). Retrieved from https://www.standard.no/fagomrader/energi-og-klima/petroleum/norsok-standards/#.WEr3QdV9600

2. A Short Introduction to Corrosion and Its Control. (n.d.). Retrieved from http://www.npl.co.uk/upload/pdf/basics_of_corrosion_control.pdf.

3. Al Khamis, M. N., Al Khalewi, F. T., Al Hanabi, M., Al Yateem, K., Al Qatari, A., & Al Muailu, H. (2014, January 19). A Comprehensive Approach of Well Integrity Surveillance. International Petroleum Technology Conference. doi:10.2523/17465-MS

4. AlAjmi, M. D., Abdulraheem, A., Mishkhes, A. T., & Al-Shammari, M. J. (2015, March 3). Profiling Downhole Casing Integrity Using Artificial Intelligence. Society of Petroleum Engineers. doi:173422-MS

5. Al-Ajmi, M.F. Juma, A.K., and Alex, Daye 2003. North Kuwait Down-hole Corrosion Management Challenge and the Use of New Corrosion Detection Tools to Define the Extent of the Problem. Paper SPE 81442 presented at the SPE 13th Middle East Oil Show & Conference, Bahrain, April 5-8 2003.

6. Al-Ashhab, J., Afzal, M., & Emenike, C. O. (2004, January 1). Well Integrity Management System (WIMS). Society of Petroleum Engineers. doi:10.2118/88696-MS

7. Al-Yateem, K.S. Le Kohring, and Qahtani, H.B. et al. 2013. Measuring and Profiling Casing Corrosion for Predicting Subsurface Leaks. Paper SPE 17170 presented at the International Petroleum Technology Conference, Beijing, China, March 26-28 2013.

8. Brill, T. M., Demichel, C., Nichols, E. A., & Zapata Bermudez, F. (2011, January 1). Electromagnetic Casing Inspection Tool for Corrosion Evaluation. International Petroleum Technology Conference. doi:10.2523/14865-MS

9. Brill, T. M., Le Calvez, J.-L., Demichel, C., Nichols, E., & Bermudez, F. Z. (2011, January 1). Quantitative Corrosion Assessment with an EM Casing Inspection Tool. Society of Petroleum Engineers. doi:10.2118/149069-MS

10. Brill, T.M. Le Calvez, J.L., and Bermudez, F. Z. 2011. Electromagnetic Casing Inspection Tool for Corrosion Evaluation. Paper SPE 14865 presented at the International Petroleum Technology Conference, Bangkok, Thailand February 7-9 2012.

11. Burton, J. P., & Yang, H. (2011, January 1). Outer Concentric String Casing Damage Evaluation: Advancements in Electromagnetic Inspection Data Interpretation for Common North Slope Well Completions. Society of Petroleum Engineers. doi:10.2118/144575-MS

12. Considine TJ, Watson RW, Considine NB, Martin JP. Environmental regulation and compliance of Marcellus Shale gas drilling. Environ Geosci.2013;20-1:16.

13. Corrosion & Environmental Degradation. (n.d.). Retrieved from https://www.princeton.edu/~maelabs/mae324/12/introduction.htm

14. Corrosion Basics, An Introduction, L.S. Van Delinder, ed. (Houston, TX: NACE, 1984).

15. Corrosion. (2012). Retrieved from http://2012books.lardbucket.org/books/principles-of-general-chemistry-v1.0/s23-06-corrosion.html

16. Cuthbert, J. F., & Johnson, W. M. (1974, January 1). New Casing Inspection Log. Society of Petroleum Engineers. doi:10.2118/5090-MS

17. Davies RJ, et al. Oil and gas wells and their integrity: Implications for shale and unconventional resource exploitation. Mar Pet Geol. 2014 doi: 10.1016/j.marpetgeo.2014.03.001.

18. Different Types of Corrosion. (n.d.). Retrieved from http://www.corrosionclinic.com/types_of_corrosion/crevice_corrosion.htm

19. Edwards, J. M., & Stroud, S. G. (1964, April 1). Field Results of the Electromagnetic Casing Inspection Log. Society of Petroleum Engineers. doi:10.2118/664-PA

20. Factors which affect corrosion. (n.d.). Retrieved 2011, from http://www.emedicalprep.com/study-material/chemistry/electro-chemistry/factor-affecting-corrosion.html

21. Ingraffea AR, Wells MT, Santoro RL, Shonkoff SBC. Assessment and risk analysis of casing and cement impairment in oil and gas wells in Pennsylvania, 2000–2012. Proc Natl Acad Sci USA. 2014;111:10955–10960.

22. Loveland, M.J. and Burton, Joey 2007. Well Integrity Assurance: A Successful Method for External Corrosion and Damage Detection on Outer and Middle Concentric Strings of Casing. Paper SPE 108698 presented at the 2007 SPE

Annual Technical Conference and Exhibition, Anaheim, California, U.S.A., Novermber 11-14 2007.

23. Oliver, D. (2004, January 1). New Slimline Electromagnetic Casing Inspection Technology. Society of Petrophysicists and Well-Log Analysts.

24. PipeView Multifinger Caliper Tool. (n.d.). Retrieved from http://www.slb.com/services/well_intervention/slickline/pipeview.aspx

25. Rourke, M., Li, Y., & Roberts, G. (2013, March 26). Multi-Tubular Corrosion Inspection Using a Pulsed Eddy Current Logging Tool. International Petroleum Technology Conference. doi:10.2523/16645-MS

26. Saudi Aramco Well Integrity Surveillance Manual. (2012).

27. Sharshar, A. E., Nutt, R. L., Smith, P. M., & Crossouard, P. A. (1991, January 1). Dukhan Field Multiwell Corrosion Study. Society of Petroleum Engineers. doi:10.2118/21366-MS

28. Smith, G. S. (1981, January 1). Principles And Applications Of A New In-Situ Method For Inspection Of Well Casing. Society of Petroleum Engineers. doi:10.2118/9634-MS

29. Stroud, S. G., & Fuller, C. A. (1962, March 1). New Electromagnetic Inspection Device Permits Improved Casing Corrosion Evaluation. Society of Petroleum Engineers. doi:10.2118/115-PA

30. Szary, T. (2006). The Finite Element Method Analysis for Assessing the Remaining Strength of Corroded Oil Field Casing and Tubing (Unpublished master's thesis). Universität Bergakademie Freiberg.

31. Torbergsen, H. B. (n.d.). Introduction to Well Integrity. doi:https://www.norskoljeoggass.no/Global/2013 Dokumenter/Andre vedlegg/introduction to well integrity - 04 December 2012.pdf

32. Vidic RD, Brantley SL, Vandenbossche JM, Yoxtheimer D, Abad JD. Impact of shale gas development on regional water quality. Science.2013;340(6134):1235009.

33. Vignes, B., & Aadnøy, B. S. (2010, May 1). Well-Integrity Issues Offshore Norway. Society of Petroleum Engineers. doi:10.2118/112535-PA

34. Watson TL, Bachu S. Evaluation of the potential for gas and CO_2 leakage along wellbores. SPE Drill & Compl. 2009;24:115–126.

35. Winning, I., Taylor, A., & Ronceray, M. (2010, January 1). Corrosion Mitigation - The Corrosion Engineers Options. Society of Petroleum Engineers. doi:10.2118/130299-MS

36. Zhang, S. “Peter,” Guergueb, N., Garcia, J., Yateem, K. S., & Sethi, N. (2013, March 26). Successful Application of a New Electromagnetic Corrosion Tool for Well Integrity Evaluation in Old Wells Completed with Reduced Diameter Tubular. International Petroleum Technology Conference. doi:10.2523/16997-ABSTRAC

VITAE

Name	Mohammed Dhafer Mohammed Al-Ajmi
Nationality	Saudi
Email	Mohad-2004@hotmail.com
Mailing Address	P.O. Box 310 - 31311 Aramco, Abqaiq, Saudi Arabia
Education	B.Sc. in Petroleum Engineering from KFUPM – 2012
Professional Experience	North Ghawar Water Injection Engineering Unit, Saudi Aramco, July, 2012 to July, 2013 Southern Area Field and Well Services Operations, Saudi Aramco, July, 2013 to April, 2014 North Ghawar Water Injection Engineering unit, Saudi Aramco, April, 2014 to July, 2014 North Ghawar Technical Support Unit, Saudi Aramco, July, 2014 to July, 2015 Ain Dar Production Engineering Unit, Saudi Aramco, July, 2015 to present.
Publications	1. SPE-182817-MS (Model assisted examination of disposal system capacity based on injected water quality). 2. SPE-181333-MS (Leveraging single phase characteristics of water injectors to optimize reservoir pressure surveillance). 3. SPE-182758-MS (Field Application of Electromagnetic Eddy Current Technology enables proactive near surface casing inspection). 4. SPE-182818-MS (Field Application of Glass Reinforced Epoxy GRE Coating in Water Injection Wells Resolves Reoccurrence of Tubing Failures). 5. SPE-182798-MS (Feasibility Study of Utilizing Hydraulic Turbines to Recover Excess Power from Water Injection Systems). 6. SPE-182236-MS (Strategies for Early Detection of Downhole Casing Failures Caused by Corrosive Formations). 7. SPE-184776-MS (Electric-Line Milling Operation on Tree Master Valve of a High Surface Pressure Well Enables Well Control).